Identifying Major Phosphorus Pathways in the Lake Michigan Nearshore Zone

Contract M03029P05

Final Report Submitted to the
Milwaukee Metropolitan Sewerage District

by

Harvey A. Bootsma[1]
James T. Waples[1]
Qian Liao[2]

[1]School of Freshwater Sciences
Great Lakes WATER Institute
University of Wisconsin-Milwaukee

[2]Department of Civil Engineering and Mechanics
Great Lakes WATER Institute

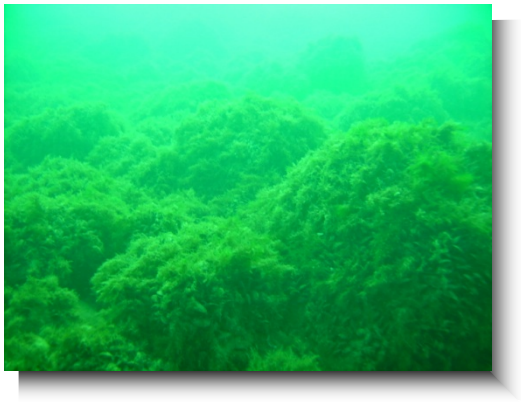

January, 2012

UNIVERSITY of WISCONSIN UWMILWAUKEE

GREAT LAKES WATER INSTITUTE

MMSD Preserving The Environment • Improving Water Quality

Identifying Major Phosphorus Pathways in the Lake Michigan Nearshore Zone

Final Report

MMSD Contract M03029P05

Harvey A. Bootsma[1]
James T. Waples[1]
Qian Liao[2]

[1]School of Freshwater Sciences
University of Wisconsin-Milwaukee
600 E. Greenfield Ave.
Milwaukee, WI 53204

[2]Department of Civil Engineering and Mechanics
University of Wisconsin-Milwaukee
Milwaukee, WI 53201

Submitted to the Milwaukee Metropolitan Sewerage District

January, 2012

Table of Contents

Acknowledgements

The work reported here was conducted with support from the Milwaukee Metropolitan Sewerage District. We are particularly grateful for the assistance of Mr. Christopher Magruder (MMSD), who provided valuable input at the project design phase and constructive reviews during the project reporting phase. We are also grateful to the captain and crew of the *RV Neeskay*, who provided invaluable technical support for our field work. We also acknowledge the assistance of Ms. Erin Wilcox, who conducted all nutrient analyses, and Mr. Leonardo Gutierrez, who performed much of the nearshore hydrodynamic modeling under the guidance of Q. Liao. The quality of this report was greatly improved following reviews by C. Magruder and T. Bate.

Terminology

Phosphorus is a nutrient that plays a criticial role in the dynamics of *Cladophora* and other algae in Lake Michigan. Phosphorus occurs in numerous forms in aquatic ecosystems. In the literature, the nomenclature for these different forms is not always consistent, and this can lead to confusion when comparing different reports. Below is a summary of the phosphorus terminology used in this report, along with definitions of other technical terms.

Clearance Rate. The effective volume of water from which all edible, particulate material is removed by mussels over a given period of time. Typical units are L $hour^{-1}$ (liters per hour), or m^3 day^{-1} (cubic meters per day). In practice, clearance rate is usually determined as the grazing rate (mass per time) divided by the concentration of particulate material (mass per volume).

Dissolved Organic Phosphorus (DOP). Dissolved organic phosphorus may include a large suite of phosphorus-containing molecules that either leach from or are excreted by biota, including nucleic acids, phosphoproteins, phosphate esters, and nucleotide phosphates (ADP, ATP). Some algae, including *Cladophora*, are capable of utilizing DOP by producing an enzyme, **alkaline phosphatase**, which hydrolyses organic phosphorus to produce PO_4^{3-}, which is then taken up and assimilated. DOP concentration is usually determined indirectly, by subtracting the SRP concentration from the TDP concentration.

dpm. Disintegrations per minute, which is a measure of radioactive decay of a substance.

Egestion. The release of particulate feces following digestion.

Ejecta. Particulate material released by mussels. It includes both feces (excreted via the anus) and pseudofeces (ejected from the mussel's incurrent siphon).

Excretion. The release of dissolved material following digestion.

Flux. The rate at which a substance, such as phosphorus, moves from one pool to another (e.g. particulate to dissolved), or one location to another (e.g. water column to the lake bottom, or vice versa). Units are usually mass per unit area per unit time.

Grazing Rate. The amount (mass) of material removed from the water column by mussels over a given time period. Units can be expressed as mass per unit time (e.g. mg day^{-1}) or, if normalized to lake bottom area, as mass per unit area per unit time (e.g. mg m^{-2} day^{-1}). Grazing rate is equivalent to **filtration rate**.

Isobath. A contour of the lake bottom that follows a constant depth.

Limiting Nutrient. The dissolved nutrient that is least available relative to the amount required by algae. In Lake Michigan, and most regions of the Great Lakes, phosphorus is usually the limiting nutrient. As a result, algae growth responds more to fluctuations of dissolved phosphorus concentration than it does to other nutrients.

Nearshore Zone. There is no strict definition of the nearshore zone of a lake. Rather, the definition is usually functional, and specifically related to the topic being studied. For the purpose of this study, the boundary between the nearshore zone and offshore zone is defined as the depth at which the summer thermocline makes contact with the lake bottom, which is usually 20 – 30 m.

Offshore Zone. The portion of the lake in which the bottom depth is below the thermocline. Both the offshore zone and the nearshore zone can be vertically separated into the water column and the lake bottom (**benthos**).

Particulate Phosphorus (PP). This is the phosphorus present in particulate material that is collected on a filter. The definition of "particulate" depends on the pore size of the filter that is used. In this study, all filtration was done using Whatman GF/F glass fiber filters, which have a nominal pore size of about 0.7 μm. Particulate phosphorus may include organic phosphorus within organic detritus, mineral phosphorus resulting from precipitation (often with iron or calcium), and phosphorus that is adsorbed onto the surfaces of particles. PP is measured by combusting filtered samples, followed by digestion in acid to convert all P to PO_4^{3-} (orthophosphate), which is measured using the molybdate method.

Pelagic. The open waters of a lake. This includes offshore zone, but does not include the lake bottom of the offshore zone.

Phosphorus (P). A non-metal element with a molecular weight of 30.97 g mol^{-1}. It is required by all bacterial, plant and animal life. In many temperate lakes, including Lake Michigan, phosphorus is the nutrient that is present in the lowest concentraton relative to the demand by algae. Therefore phosphorus is referred to as a "limiting nutrient" in these lakes.

Pseudofeces. Particulate material that is ejected from a mussel's incurrent siphon. It is made up of particulate material that is ingested by the mussel, but not digested. The material is wrapped in a mucous coating and "spat" back out of the same opening (the incurrent siphon) through which it entered.

Seston. All particulate material suspended in water. In practice, the size range is usually between 1 μm and 1 mm.

Soluble Reactive Phosphorus (SRP). This is dissolved phosphorus that is measured by reaction with molybdate (the reaction produces a blue color, which is measured using a spectrophotometer). This method was designed to measure the orthophosphate ion (PO_4^{3-}), which is the form of phosphorus that is most directly available to algae. However, the analytical procedure may result in the hydrolysis of some organic phosphorus to PO_4^{3-}, which can result in an overestimate of the PO_4^{3-} concentration. Therefore, while the method is believed to provide an estimate of the amount of dissolved phosphorus that is directly available to algae, in practice it is more correct to refer to the measured form of phosphorus as soluble reactive phosphorus.

Thermocline. The depth at which temperatures rapidly change during the stratified period (usually from May to November). The thermocline separates warm surface water from colder bottom water. In Lake Michigan, the summer thermocline depth is usually between 20 and 30 meters.

Tissue Phosphorus. This refers to the phosphorus concentration within algae tissues, sometimes called the internal P content. It is a useful measurement because it directly controls algae growth rates. It is usually presented with units of μg P $mgDW^{-1}$, where mgDW is the milligrams of dry weight of *Cladophora*. Some literature uses units of %. The % P content is equal to μg P $mgDW^{-1}$ divided by 10. Tissue phosphorus is sometimes referred to as the **cell phosphorus quota**, designated as **Q**.

Total Dissolved Phosphorus (TDP). For the purpose of this study, TDP is all phosphorus that passes through a filter with a 0.7 μm pore size. It includes both dissolved organic phosphorus and dissolved inorganic phosphorus. TDP is measured by photo-oxidizing water samples under acidic conditions in the presence of peroxide, which converts all P to PO_4^{3-}. Total dissolved phosphorus is sometimes referred to simply as **dissolved phosphorus (DP)**.

Total Phosphorus (TP). This include all forms of phosphorus. From both a functional and an analytical perspective, total phosphorus can be divided into two main categories – particulate and dissolved.

1. Executive Summary

1. This study provides the first ecosystem-scale analysis of phosphorus dynamics within the nearshore zone of Lake Michigan (or any Great Lake). The paradigm that emerges is one in which mussels have accelerated the rate at which particulate material is deposited on the lake bottom, changing the phosphorus content of this material as they graze and digest it. The net effect is to alter the balance of nutrient flow between the nearshore and offshore (pelagic) zones, so that the nearshore zone has become a net sink for phosphorus. This sink is particularly strong during the summer months, when large amounts of this phosphorus are incorporated into mussel tissue and *Cladophora* tissue.

2. This study suggests that, for nearshore regions other than those immediately adjacent to tributary rivers, **the offshore zone is a more significant source of phosphorus than direct loading from tributaries on a short term (annual) time scale.** The measurement of particulate P fluxes between offshore and nearshore zone indicate that this exchange is relatively large. **For example, for a 10 km stretch of shoreline in the Milwaukee region, particulate P derived from the offshore zone may be up to three times greater than the P loading from Milwaukee Harbor to the lake.** Estimates of mussel grazing rates indicate that the mussel community has the capacity to graze virtually all of the particulate P that is derived from the offshore zone. Previous measurements (Bootsma et al. 2008a) also **indicate that P recycled by mussels is sufficient to support all of the *Cladophora* growth that occurs in the nearshore zone.**

3. The influence of mussel metabolism on algal abundance in Lake Michigan can be evaluated by examining the carbon:phosphorus (C:P) ratio of various nutrient pools. Because phosphorus is the limiting nutrient for algae in Lake Michigan, the amount of phosphorus available to algae will determine the amount of carbon, or biomass, that the algae are able to produce. Mussels tend to release C and P at a ratio similar to that of the phytoplankton on which they feed. However, *Cladophora* tends to have a much higher C:P ratio, almost two times greater than that of phytoplankton. This reflects the ability of *Cladophora* to grow on very low concentrations of phosphorus. **As a result, the phosphorus that is excreted by mussels (which is derived primarily from the consumption of phytoplankton) can potentially lead to the**

production of *Cladophora* biomass that is twice as great as that of the phytoplankton from which the phosphorus originated.

4. The results of this study support those of a previous study (Bootsma et al. 2008a), which concluded that mussel-mediated recycling of phosphorus in the nearshore zone is large relative to loading from the Milwaukee Harbor. **The potential importance of the offshore (pelagic) zone as a nutrient source for the nearshore zone means that phosphorus supply to the nearshore zone will respond to management actions only as fast as the entire lake responds.** Whole-lake models (Pauer et al. 2007) indicate that, following a change in nutrient loading, it takes approximately 10 years for a new steady state to be reached in Lake Michigan. These same models suggest that a 50% reduction in phosphorus loading should lead to a reduction in total phosphorus (TP) concentration from ~4.5 ug/ L to between 3 and 3.5 ug/ L. However, these models do not account for the effect of dreissenid mussels. **Currently the offshore (pelagic) TP concentration is between 2 and 4 ug/L,** and there is strong evidence that mussel filter feeding is at least partly responsible for the relatively rapid decline in TP concentration over the past two decades. Until the whole-lake models are revised to account for mussels, it is difficult to determine exactly how whole-lake TP concentration will respond to any further decrease in P loading. But even at the current low TP concentrations, mussels are very effective at concentrating P within the nearshore zone, especially near the benthos where it can be utilized by *Cladophora*. **This efficient concentration mechanism will make it difficult to achieve *Cladophora* control through management of P loading, and it is likely that, as long as high concentrations of dreissenid mussels persist in the nearshore zone, *Cladophora* and other benthic algae will continue to grow at nuisance levels.**

2. Introduction and Background

Research conducted over the past four years has helped to identify the causes of excessive growth of the nuisance alga, *Cladophora* sp., in the Milwaukee region of Lake Michigan. A review of historic water quality conditions in this region indicates that average summer nearshore water temperatures have increased by about 2.5^{o}C since 1990, water clarity is approximately twice as great as it was in the early 1990s, and there appears to have been a small increase in the concentration of dissolved phosphorus (Auer et al. 2010). The potential effect of these changes on *Cladophora* growth and biomass has been tested by using a calibrated *Cladophora* model to simulate *Cladophora* growth and biomass for the period immediately prior to invasion by the exotic dreissenid mussels, the zebra mussel (*Dreissena polymorpha*) and the quagga mussel (*Dreissena bugensis*), and the post-invasion period. These simulations indicate that increased water clarity is the primary factor responsible for increased algal growth and biomass over the past fifteen years, with the increase in dissolved phosphorus concentration being a secondary contributing factor (Auer et al. 2010; Tomlinson et al. 2010).

Although light appears to be the primary factor contributing to excess *Cladophora* growth in the Milwaukee region of Lake Michigan, nearshore water clarity is not a property that can be managed directly. Rather, the supply of nutrients, especially phosphorus, is the only mechanism by which *Cladophora* growth might be managed. To date, nutrient management for Lake Michigan has focused on reducing total phosphorus concentrations to a level at or below a target of 7 μg L^{-1}, as prescribed in the Great Lakes Water Quality Agreement. For the open waters of the lake, and for at least parts of the nearshore zone, this target has been achieved, with reported concentrations of between 2 and 4 μg L^{-1} (State of the Great Lakes 2009; Mida et al. 2010). But the persistence of high *Cladophora* biomass under these conditions suggests that the relationship between phosphorus loading and nearshore algae needs to be re-examined, and nearshore phosphorus targets may need to be reconsidered.

Previous research has indicated that dreissenid mussels themselves are a significant source of dissolved phosphorus in the nearshore zone of Lake Michigan, because a significant amount of the particulate phosphorus they ingest is digested and excreted in dissolved form (Bootsma et al. 2008a; Bootsma 2009). Hence the mechanisms that control phosphorus availability and, ultimately, *Cladophora* growth in the nearshore zone are markedly different from those that operated prior to the dreissenid mussel invasion. The phosphorus targets specified in the Great Lakes Water Quality Agreement were determined based on models that reflected the understanding of nutrient cycling processes in the Great Lakes in the 1970s. Similarly, new management strategies for nutrients and nuisance algae in the nearshore zone must be based on a solid understanding of the mechanisms that control nutrient supply and algal growth.

To the extent possible, this understanding needs to be captured in numerical models, which serve both to test the validity of hypothesized mechanisms and to assist in the development of management strategies.

The need to understand nearshore zone phosphorus dynamics is especially relevant at the present time, as the State of Wisconsin has adopted new phosphorus standards for inland lakes and rivers, and for discharge from industries and waste water treatment plants. Limits have been established at 0.1 mg L^{-1} for select rivers/creeks/harbors, 0.075 mg L^{-1} for all other streams and 0.007 mg L^{-1} for open waters of Lake Michigan (WDNR 2010a). Also, on July 1, 2010 the State of Wisconsin enacted a law limiting the phosphate content of dishwashing detergent to 0.5% or less (WDNR 2010b).

While phosphorus abatement has been an effective strategy for reducing nuisance algae growth in the Great Lakes in the past four decades, changes in the biological communities of the Great Lakes, especially within the nearshore zone, has resulted in changes in phosphorus cycling dynamics (Hecky et al. 2004). For example, previous research has shown that, in the nearshore zone of Lake Michigan near Milwaukee, phosphorus excretion by quagga mussels is several times greater than the phosphorus loading from the Milwaukee River (Bootsma et al. 2008a). This new paradigm needs to be taken into account when considering the potential benefits of the proposed new phosphorus limits.

3. Objectives

The research conducted to date has quantified the amount of dissolved phosphorus that is supplied by dreissenid mussels in the nearshore zone, and has examined some of the environmental factors that may influence this supply rate, including temperature, food supply, and mussel size. These data have been used to develop a preliminary empirical phosphorus excretion model. In order to be used as a management tool, this model needs to be incorporated into a larger conceptual model of phosphorus dynamics in the nearshore zone. A diagram of this conceptual model is presented in Fig. 1. As highlighted in the model, a number of phosphorus cycling processes are moderately well understood, while others remain unstudied. In particular, the following questions need to be addressed:

3.1. What is the source of food for dreissenid mussels? Ultimately, the supply of dissolved phosphorus from mussels is dependent on the amount of food (which contains particulate phosphorus) that is available to the mussels. Potential sources include seston (suspended particulate material, including algae) from river loads, resuspension of bottom sediments, wastewater treatment effluent discharge, and transport of offshore zone seston (including plankton) shoreward into the nearshore zone. The relative importance of these various food sources will determine how quickly *Cladophora* will respond to any changes in phosphorus loads to the lake. For example, if a large proportion of dreissenid

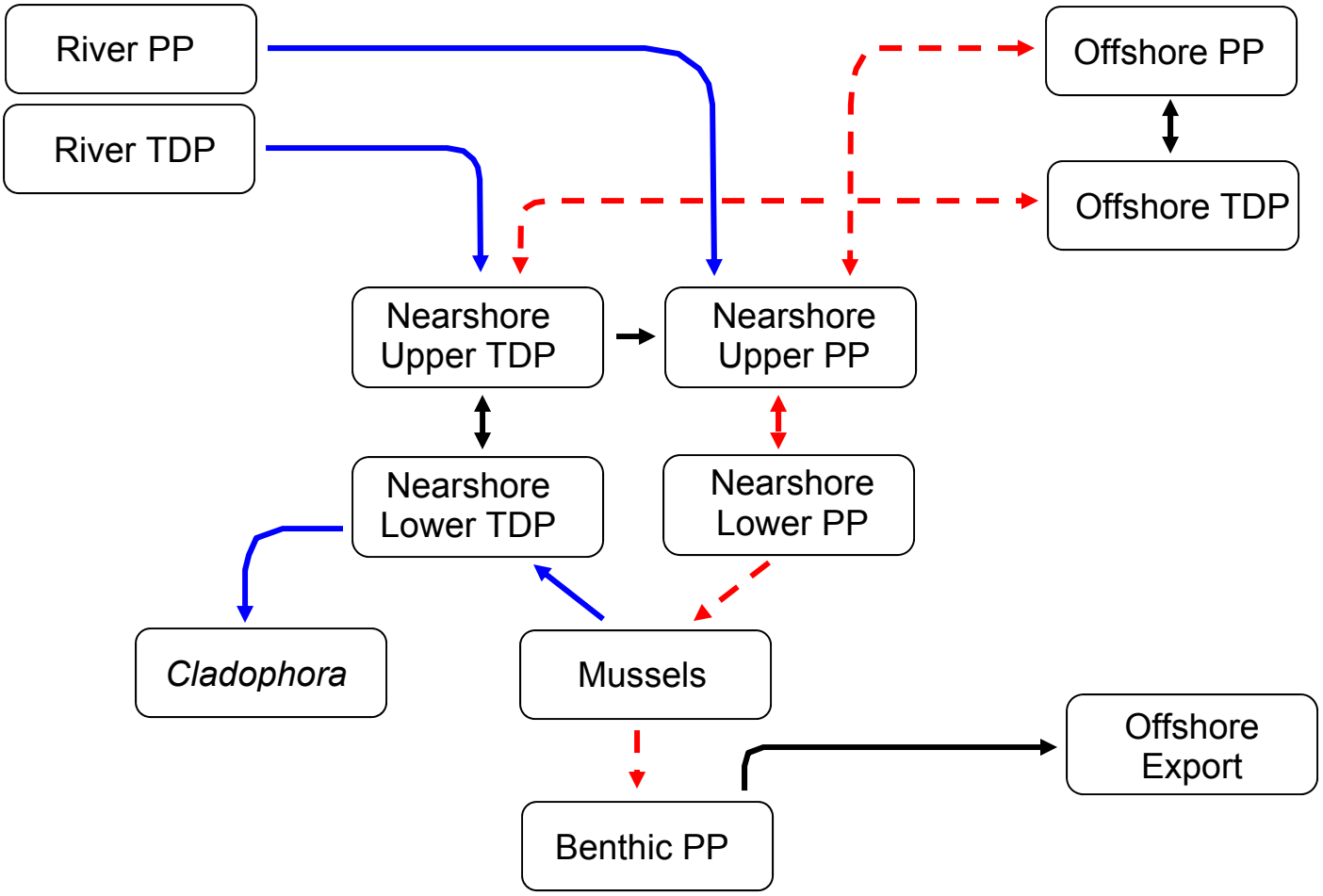

Fig. 1. Conceptual model of phosphorus dynamics in the Lake Michigan nearshore zone. Solid-line pathways are those that are moderately well understood, based on research conducted over the past four years. Dashed pathways are those that are poorly understood. In the nearshore zone, "Upper" refers to the water column, and "Lower" refers to the benthic boundary layer (several cm above the lake bottom). PP = particulate phosphorus; TDP = total dissolved phosphorus.

food comes directly from river loading, then *Cladophora* will respond quickly to any reduction in river P loading. But if dreissenids rely heavily on offshore plankton as a food source, *Cladophora* response to reduced river loading will be slower because the lake as a whole responds slowly to changes in external nutrient loading.

3.2. What are the physical exchange rates between the nearshore and offshore zones? This question must be adressed in order to answer question 1, as the supply of seston from the offshore to the nearshore zone is controlled by physical exchange rates.

3.3. What is the fate of phosphorus excreted / egested by mussels? Mussels release both dissolved and particulate forms of phosphorus. A significant portion of the particulate phosphorus released by mussels is in the form of feces and pseudofeces, but the ability of this form of phosphorus to support *Cladophora* growth is not known. If it is eventually recycled and converted to a dissolved form within the nearshore zone, then it can support algal growth, but if it remains in a particulate form that is eventually transported to the offshore zone where it is buried, it will not support *Cladophora* growth.

3.4. What is the flux rate of particulate and dissolved phosphorus between the water column and the lake bottom (benthos) in the nearshore zone? Mussels excrete large amounts of dissolved phosphorus, but the availability of this phosphorus to benthic *Cladophora* will depend on vertical mixing rates in the water column. If these mixing rates are high, excreted dissolved phosphorus will be diluted into the water column before it can be assimilated by *Cladophora*, but if mixing rates are low, much of this dissolved phosphorus may be taken up by *Cladophora*. Likewise, vertical mixing rates can control food supply to mussels. Under low mixing conditions, the bottom layer of water can become seston-depleted due to mussel filtration (grazing), so that mussels become food-deprived. Under high mixing rates, food in the bottom layer will be continually replenished by mixing from above. Parameterizing the links between mixing, food supply and dissolved phosphorus flux is critical to modeling phosphorus dynamics and *Cladophora* growth in the nearshore zone.

The general objective of this study was to address the above questions in order to provide an understanding of phosphorus cycling dynamics at the ecosystem scale within the nearshore zone of Lake Michigan, (i.e. to understand how individual phosphorus cycling processes such as river loading, mussel feeding and excretion, settling, resuspension, and nearshore-offshore water exchange combine to regulate nearshore phosphorus concentrations and nuisance *Cladophora* growth). **From a management perspective, the ultimate goal is to predict how nuisance algal growth will respond (decline) to changes (reductions) in phosphorus loading.**

4. Approach

Previous research (Bootsma et al. 2008a) focused on individual phosphorus cycling processes, including river loading, excretion by mussels, and *Cladophora* growth. To place these processes into a larger, more complete ecosystem context, the present study used several different approaches to acquire an integrated measure of phosphorus flow through the Lake Michigan nearshore zone. The core of this study consisted of an intensive one-month field experiment on a rocky reef several kilometers south of Milwaukee, referred to here as "Green Can Reef" (because of the presence of a large, green navigational buoy near this site; Fig. 2). Aerial images and underwater surveys indicate that this region is dominated by rocky substrate, which is thickly covered with quagga mussels and *Cladophora*. The specific goal of this field study was to measure a number of phosphorus fluxes in order to identify the dominant phosphorus flow pathways in the nearshore zone, and to better define the quagga mussel's role within this context.

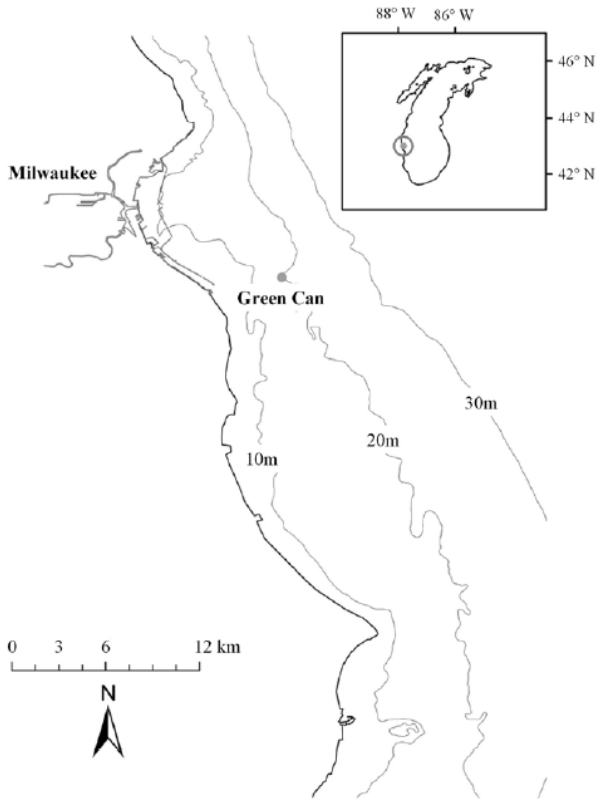

Fig. 2. Location of the Green Can study site south of Milwaukee Harbor. Lat: 42^{o} 59.1600' N. Long: 87^{o} 47.9284' W.

Specific measurements made during this intensive study included:

4.1 Consumption of particulate phosphorus and excretion of dissolved phosphorus by quagga mussels (measured *in situ*). These measurements were made using two methods: deployment of benthic incubation chambers on the lake bottom at a depth of 20 meters, and deployment of an *in situ* particle image velocimetry (PIV) system.

For benthic chamber experiments, prior to deployment, all benthic algae were removed from the incubation site. Chambers were sealed to the rocky substrate with neoprene skirts weighted with lead-shot socks (see Appendix I Fig. A1.1 for images). Dissolved phosphorus excretion (SRP and TDP) was determined by collecting water samples from the chambers at the beginning and end of an incubation period of 1 to 3 hours. Excretion rates were normalized to both rock surface area and mussel biomass within the incubation chambers. The purpose of these measurments was to determine how important quagga mussel P excretion rates are within the context of other major P flux pathways in the nearshore zone.

PIV technology provides a non-intrusive method of measuring small-scale hydrodynamics in the near-bottom layer of water, just above the mussel bed. When combined with measurements of the vertical profiles of particulate material and dissolved phosphorus within this same layer (which are made with a separate microprofile sampler), these measurements can be used to derive vertical fluxes of these components, i.e. downard flux of particles (or upward flux during resuspension events), and upward flux of dissolved P excreted by mussels. A detailed description of the method is provided by Liao et al. (2009).

4.2 Net sinking rates of particles and phosphorus in the nearshore zone, as derived with the radionuclide tracers. Naturally occurring radionuclide parent / daughter pairs were used to determine settling rates. The first is the Thorium / Uranium pair (^{234}Th/^{238}U), which allows for the measurement of particle removal rates on time scales of days to weeks. The second is the Ytrium / Strontium pair (^{90}Y/^{90}Sr), which provides a measurment of particle removal rates on time scales of hours to days. Radionuclide tracers are powerful tools in that they allow for the non-intrusive measurement of net particle loss rates, which is impossible to do with conventional approaches such as the use of sediment traps. When compared with measurements of P flux through quagga mussels, the radionuclide approach provides a measure of the importance of mussels as a conduit for P within the nearshore zone. Details about the application of radionuclide in aquatic particle flux studies are provided in Waples et al. (2003) and Waples and Orlandini (2011).

4.3 Current speed and direction. These measurments were made at the study site throughout the water column (from lake surface to lake bottom) using a

1000 kHz SonTek Acoustic Doppler Current Profiler (ADCP). The ADCP was set up to measure current speed and direction at 1-meter depth intervals every 10 minutes, with 1-minute averaging periods. These measurements were used to validate a 3-dimensional Finite-Volume Coastal Ocean Model (FVCOM; Chen et al., 2003). The model was then used to quantitatively assess the hydrodynamic exchange between the nearshore and offshore zones. The boundary between these two zones was operationally defined as the 20-meter isobath, as this is the approximate lower depth limit of *Cladophora* growth in Lake Michigan. The summer thermocline prevents direct interaction between the water column and lake bottom at depths greater than ~20 m. Because the movement of water between the nearshore and offshore zones is highly variable over space and time, there is no effective way to directly measure this exchange with *in situ* instruments. A very large array of instruments would be required, which was beyond the limitations of this study. A calibrated 3-dimensional model is the most effective approach to determining exchange rates integrated over space and time.

4.4 Supporting water quality measurements. Additional data were collected by deploying a monitoring buoy that included temperature loggers at 2-meter depth intervals, and water quality sondes located 1 m below the surface and 1 m above the lake bottom. Each sonde measured temperature, dissolved oxygen, pH, chlorophyll fluorescence (as an index of phytoplankton abundance), and turbidity (as an index of suspended particulate material). In addition, high-resolution vertical profile measurements of the same variables were made on each sampling date using a SeaBird conductivity-temperature-depth (CTD) instrument.

5. Results and Discussion

This section provides the main findings that resulted from the measurements described above. Detailed results for each of the three main study components (phosphorus excretion, radionuclide tracers measurements, and hydrodynamic modeling), along with more detailed descriptions of the methods used, are provided below in Appendices I, II and III.

A major objective of this project was to understand phosphorus cycling processes at the ecosystem scale within the nearshore zone, and the role of the quagga mussel within this context. Critical phosphorus pathways to consider include:

- loading from tributaries
- consumption (filter feeding) by mussels
- recycling (excretion) and egestion (as feces and pseudofeces) by mussels
- uptake by *Cladophora*

- exchange between the benthos (lake bottom) and the water column
- exchange between the nearshore and offshore zones.

Several of these processes have been addressed in a previous study (Bootsma et al. 2008a), including tributary loading, excretion by mussels, and uptake by *Cladophora*. The measurements made in this study helped us to quantify the remaining processes.

Estimates of phosphorus flux through the above pathways are presented in Table 1. A comparison of these rates reveals a number of major points:

a. The mussel grazing rate of 78 mg m^{-2} day^{-1} is comparable to the phosphorus sedimentation rate in the nearshore zone. The sedimentation rate is highly variable, as a result of fluctuations in nearshore zone particulate P concentration and mixing conditions. However, a grazing rate that is intermediate within the sedimentation rate range suggests that a large fraction of the particulate material that is transferred from the water column to the benthos is filtered by quagga mussels, as opposed to passively sinking to the benthos. It is likely that this processing of particulate P by mussels facilitates P recycling. Because P strongly adsorbs to particles and is released very slowly under aerobic conditions, passive settling of particles is likely an effective method of removing P from the water column (Brooks and Edgington 1994). In contrast, digestion of particulate P by mussels is an effective method of converting particulate P to dissolved P, most likely due to digestive enzymes and anaerobic conditions in the mussel digestive tract (Hecky et al. 2004).

b. Phosphorus grazed by mussels has three possible fates: excretion in dissolved form, egestion in particulate form as feces / pseudofeces, or assimilation into mussel tissue. The values in Table 1 suggest that excretion rates and egestion rates are similar in magnitude. However, the sum of these two rates is less than the estimated grazing rate. While some of the grazed phosphorus will be allocated to tissue growth, this is unlikely to make up the balance between grazing and excretion plus egestion, as a relatively small fraction of food eaten by mussels is actually assimilated (Stoeckmann and Garton 1997). The discrepancy is more likely due to an underestimate of egestion rate. The egestion rate is based on the mass of ejecta produced by mussels over a 12-hour period. In fact, mussels probably evacuate their gut contents over a much shorter time, meaning a 12-hour incubation will lead to a low rate estimate. In addition, the egestion rate in Table 1 is based on a single experiment on one day, and rates averaged over multiple days may actually be greater. The grazing rate may also be over-estimated. It is based on a mussel density of 10,000 m^{-2}, (see Appendix II for data sources). However, mussel densities are highly variable in the nearshore zone, and densities of less than 5,000 m^{-2} are often measured. If a density of 5,000 m^{-2} is

Table 1. Estimates of phosphorus flux through various pathways in the nearshore zone (Milwaukee regions) of Lake Michigan.

Phosphorus Pathway	Measurement Method	P Flux Rate
Loading from Milwaukee Harbor	Monitoring of concentration and discharge (Bootsma et al. 2008a)	247 kg P day^{-1} (~6.2 mg m^{-2} day^{-1} for a 10 km stretch of shoreline*)
Sedimentation from water column to benthos	Sediment traps and radionuclide tracers (Appendix II)	8 – 235 mg m^{-2} day^{-1} (particulate P)
Grazing by quagga mussels	Radionuclide tracers and direct measurements with Particle Image Velocimetry (Appendices I and II)	78 mg m^{-2} day^{-1}** (particulate P)
Excretion by mussels	Chamber incubations and PIV measurements (Appendix I)	3.5 – 14 mg m^{-2} day^{-1} (dissolved P)
Egestion (feces and pseudofeces) from mussels	Radionuclide tracers (Appendix II)	12 – 25 mg m^{-2} day^{-1}*** (particulate P)
Offshore to nearshore	3-D hydrodynamic model (Appendix III)	19.4 mg m^{-2} day^{-1}**** (total P)

* Calculated for the 0-10 m depth range (in which most *Cladophora* growth occurs), which results in a total area of approximately 190 km^2.

** Based on a PIV-derived clearance rate of 3.9 L $mussel^{-1}$ day^{-1} (Appendix I) an areal density of 10,000 mussels m^{-2}, and a water column particulate P concentration of 2.0 μg L^{-1}.

*** Based on a radionuclide-derived mussel ejecta rate of 16.0 – 34.9 μg sediment $mussel^{-1}$ hr^{-1} (Table A2.3, Appendix II) and a particulate P : sediment ratio of 3 mg g^{-1} (Table A2.2, Appendix II).

****Assumes that the nearshore zone (0-20 m deep) is 4 km wide.

applied, the estimated grazing rate is 39 mg P m^{-2} day^{-1}, which is within the range of measured excretion plus egestion rates. While this would lessen the role of mussels as a conduit of particles from the water column to the benthos, mussel grazing is still within the range of sedimentation rates, and remains a major phosphorus pathway in the nearshore zone.

c. The results of this study support those of a previous study (Bootsma et al. 2008a), which concluded that mussel-mediated recycling of phosphorus in the nearshore zone is large relative to loading from the Milwaukee Harbor. In addition, while further measurements are required to determine the full range of egestion rates (feces and pseudofeces production), the measurements reported here indicate that egestion may be similar in magnitude to excrection of dissolved P. At present, the fate of this egested material is not well known. A critical question is whether it remains bound in particulate form, which is eventually buried and lost from

the lake, or if it is recycled to dissolved P. A recent modeling study suggests that quagga mussels have the potential to significantly increase phosphorus retention in the sediment (Cha et al. 2011). This is not due to the way in which mussels process phosphorus (they actually convert a significant amount of consumed particulate P to dissolved P). Rather, it is due to their ability to increase the transport of particulate P out of the water column through their filter feeding activity. If a significant fraction of the particulate P egested by mussels becomes buried, it would explain the recent declines in total phosphorus and plankton in the offshore waters of Lake Michigan. It has been suggested that this mechanism may be the cause of declines in forage fish such as alewife and smelt (Nalepa et al. 2009). **While further empirical data are needed to support this suggestion, it presents a management condundrum. In the nearshore zone, phosphorus reductions are required to reduce *Cladophora* abundance, but such reductions could actually exacerbate the problem of low plankton and fish biomass in the offshore zone.**

The potential influence of mussels on nearshore P recycling is underscored by sedimentation rates derived from radionuclide tracers (Appendix II). Sedimentation rates of total particulate material, derived using the ^{90}Y tracer method, reveal a balance between sedimentation rate and the benthic inventory of particulate material, i.e. the concentration of recently settled sediment on the lake bottom is what would be expected based on calculated settling rates. However, ^{90}Y-derived sedimentation rates of phosphorus are about two times greater than the benthic inventory of particulate phosphorus. This indicates that phosphorus is being lost from the benthic pool after it has settled. This is supported by a comparison of the P concentration in particulate material in the water column and in the sediment. Within the water column, the particulate P concentration is 3.7±1.2 mg g^{-1} (mean ± standard deviation; derived by dividing PP by TSM concentrations Appendix II, Table A2.1), but in the benthos the concentration is 0.77±0.0005 mg g^{-1} (derived by dividing areal PP by areal floc, Appendix II, Table A2.3). This difference may be due to grazing by quagga mussels. Grazing results in selective recycling of P, where P is removed from sedimented particulate material and returned to the water column in dissolved form that is accessible to *Cladophora* and other algae. This mechanism is supported by other studies that have reported an increase in the ratio of dissolved P : particulate P following the establishment of dreissenid mussels (Heath et al. 1995; Makarewicz 2000).

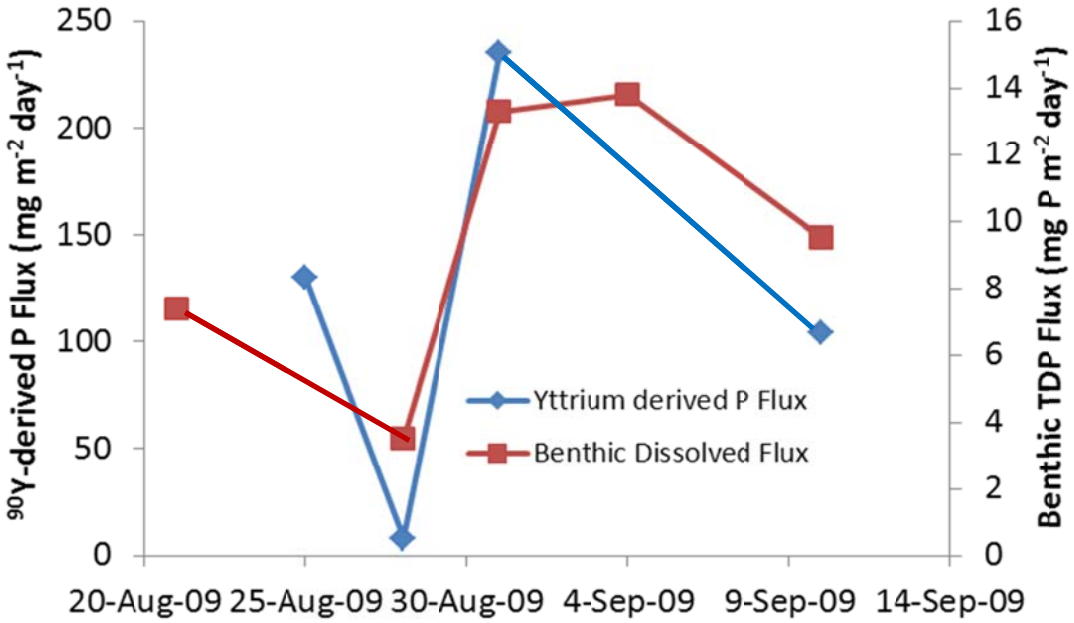

Fig. 3. Comparison of ^{90}Y-derived particulate P sedimentation rates and mussel excretion rate of total dissolved P (TDP).

The measurements made in this study allow for the comparison of particulate P sedimentation rates with dissolved P excretion by quagga mussels (Fig. 3). Sedimentation rates are an order of magnitude greater than excretion rates, indicating that a large portion of the settled P is allocated to other pools, such as particulate egestion, mussel growth, and non-mussel mediated settling. However, during the study period similar temporal patterns in settling and mussel excretion were observed (Fig. 3). This apparent link between mussel metabolism and settling suggest that either the mussels are responding to settling rates that are controlled by external mechanisms (e.g. wind-induced mixing), or settling rates are controlled by mussel metabolism (grazing). Both mechanisms are probably important. Sedimentation rates can actually be negative (i.e. resuspension events) during storm periods (Appendix II), highlighting the role of purely physical processes. But the fact that grazing rates are similar in magnitude to the settling rate (Table 1, p. 15) suggests that mussels also have the capacity to influence settling rates.

d. While the measurement of particulate P flux between offshore and nearshore zones is a technically challenging task, the preliminary estimates made in this study suggest that this flux is relatively large. For example, for a 10 km stretch of shoreline in the Milwaukee region, particulate P derived from the offshore zone may be up to three times greater than the P loading from the Milwaukee Harbor to the lake. The

estimate of mussel grazing rate indicates that the mussel community has the capacity to graze virtually all of the offshore-derived particulate P. Previous measurements (Bootsma et al. 2008a) also indicated that P recycled by mussels is sufficient to support all *Cladophora* growth that occurs in the nearshore zone. If this recycled P is derived from offshore particulate P, as the current study suggests, much of the *Cladophora* growth in the nearshore zone may be supported by the offshore phosphorus pool.

Production of offshore plankton ultimately relies on phosphorus that is loaded to the lake via the nearshore zone. Therefore, reducing P supply to the nearshore zone will require a reduction of P loading to the lake. But because the offshore plankton community represents a very large nutrient pool that is spatially diffuse and has a long turnover time, its utilization as a phosphorus source by the nearshore community means that decreases in phosphorus loading from tributaries will likely have only a marginal effect on nearshore phosphorus concentration nuisance algal abundance in the short term. Further, as long as high mussel densities persist in the nearshore zone, significant decreases in phosphorus supply to benthic algae will only result from decreases in the size of the offshore phosphorus pool.

This study provides the first ecosystem-scale analysis of phosphorus dynamics within the nearshore zone of Lake Michigan (or any Great Lake). The paradigm that emerges is one in which mussels have accelerated the rate at which particulate material is deposited on the lake bottom, changing the phosphorus content of this material as they graze and digest it. The net effect is to alter the balance of nutrient flow between the nearshore and offshore zones, so that the nearshore zone becomes a net sink for phosphorus. This sink is particularly strong during the summer months, when large amounts of this phosphorus are incorporated into mussel and *Cladophora* tissue.

Our analysis suggests that, for nearshore regions other than those immediately adjacent to tributary rivers, the offshore zone is a more significant source of phosphorus than direct loading from tributaries. This is supported by observations in other parts of Lake Michigan (e.g. Sleeping Bear Dunes National Lakeshore), where high concentrations of *Cladophora* persist in areas remote from any major tributaries.

The importance of the offshore zone as a nutrient source for the nearshore zone means that phosphorus supply to the nearshore zone will respond to management actions only as fast as the entire lake responds. Whole-lake models (Pauer et al. 2007) indicate that, following a change in nutrient loading, it takes approximately 10 years for a new steady state to be reached in Lake Michigan. These same models suggest that a 50% reduction in phosphorus loading should lead to a reduction in total phosphorus (TP) concentration from

~4.5 μg L^{-1} to between 3 and 3.5 μg L^{-1}. However, these models do not account for the effect of dreissenid mussels. Currently the offshore TP concentration is between 2 and 4 μg L^{-1}, which is below the target concentration of 7 μg L^{-1} defined in the Great Lakes Water Quality Agreement (GLWQA), and lower than what would be expected based on loading reductions alone (Mida et al. 2010). But even at the current low TP concentrations, mussels are very effective at concentrating P within the nearshore zone. This concentration mechanism may have two major impacts on Lake Michigan. First, by concentrating particulate phosphorus in the nearshore benthos and converting a significant fraction to dissolved phosphorus, *Cladophora* growth is accelerated. This effect is exacerbated by increased light availability, due to clarification of the water column by mussel filter feeding (Auer et al. 2010). Second, this same nearshore P concentration mechanism appears to be depleting P in the offshore zone, resulting in lower quantities of plankton and forage fish. These opposing impacts (too much benthic algae in the nearshore zone versus too little phytoplankton in the offshore zone) raise questions about the optimal phosphorus management strategy for Lake Michigan. The data presented here suggest that a significant proportion of the phosphorus supplied to the nearshore zone is derived from the offshore zone. In this case, significant decreases in nearshore dissolved phosphorus concentration will require decreases in offshore (i.e. whole-lake) concentrations. Such decreases can be achieved through reductions in phosphorus loading, but the response time will be slow (5 to 10 years), and it will be challenging to find ways in which P loading can be reduced below present levels, which are already below the GLWQA target level. The fact that *Cladophora* continues to thrive when total P concentrations are well below the target level of 7 μg L^{-1} underscores the efficiency of the nearshore benthic P concentration mechanism, and suggests that it may be difficult to achieve *Cladophora* control through management of P loading. As long as high concentrations of dreissenid mussels persist in the nearshore zone, *Cladophora* and other benthic algae may continue to grow at nuisance levels.

The Lake Michigan phosphorus cycle is in a state of transition. Until recently, dreissenid mussels were dominated by the zebra mussel, *Dreissena polymorpha*, which was confined to hard substratum in the nearshore zone. However, over the past decade this species has been replaced by its congener, the quagga mussel (*Dreissena rostriformis bugensis*) which is capable of colonizing soft substratum and growing at cold temperatures (Nalepa et al. 2010). Recently, evidence has emerged that filter feeding by deep, offshore communities of this species may be having a significant impact on the abundance of pelagic phytoplankton (Fahnenstiel et al. 2010; Vanderploeg et al. 2010). The deep-water mussel community continues to expand, and so its impact on pelagic phytoplankton may be expected to strengthen in the near future (Vanderploeg et al. 2010). Due to the dependence of the nearshore zone on the offshore zone as a plankton (and particulate phosphorus) source, further depletion of the offshore plankton community by filter feeding deep-water mussels may lead to lower total phosphorus concentrations and less *Cladophora* in the nearshore zone.

The strength of this interaction will depend on the degree to which spring feeding by deep-water mussels affects phytoplankton abundance later in the summer. In low-rainfall summers when external nutrient loading is low, phytoplankton production will rely heavily on internal phosphorus supplies (Brooks and Edgington 1994), which can be controlled by dreissenids. In contrast, under conditions of high river discharge and external nutrient loading, grazing by the deep-water mussel community will have a reduced effect on nearshore nutrients and *Cladophora* will respond more directly to river phosphorus loads. This may become a more common occurrence in the future if the frequency of large storm events in the Great Lakes region continues to increase (Kling et al. 2003). Under these conditions, minimizing phosphorus loss from both rural and urban watersheds will remain an important tool for minimizing *Cladophora* growth. Whether further nutrient load reductions will exacerbate the problem of low phytoplankton abundance in the offshore zone is uncertain. Whole-lake nutrient models will help to answer this question, but their predictive capacity is limited,due to the exclusion of dreissenids.

Research over the past decade has improved our understanding of the nearshore phosphorus cycle and causes of excessive *Cladophora* growth, but our knowledge of how dreissenids are affecting the offshore phosphorus cycle is very limited (Vanderploeg et al. 2010). The results of this study indicate that nearshore phosphorus concentrations and *Cladophora* growth are likely closely linked to whole-lake internal phosphorus cycling. Updated measurements and modeling of offshore phosphorus dynamics will allow for better predictions of how offshore plankton, fish communities, and nearshore *Cladophora*, will respond to changes in phosphorus loading.

Appendix I. Particulate Consumption and Phosphorus Excretion by Quagga Mussels.

Benthic Chamber Incubations

The benthic chamber used to measure *in situ* dissolved P excretion rates is shown in Fig. A1.1. In addition to collecting subsamples for dissolved P analysis, the chamber was fitted with a probe that allowed for continuous measurement of dissolved oxygen concentration, so that respiration rate and P excretion could be measured simultansously.

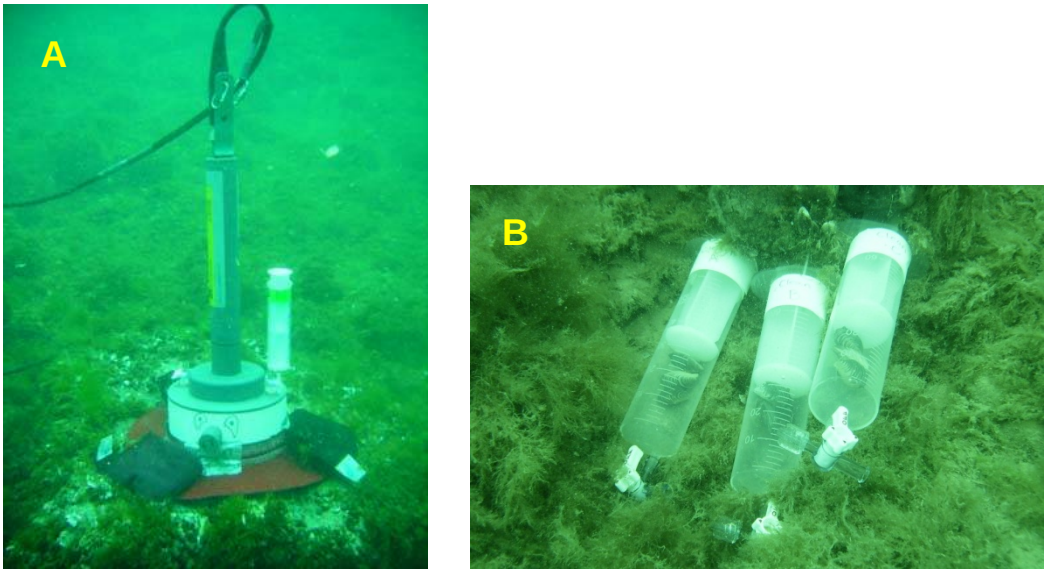

Fig. A1.1. A. Benthic chamber used to measure oxygen consumption and dissolved phosphorus excretion by quagga mussels. B. In situ syringes used to measure dissolved phosphorus excretion by mussels detached from the substrate.

An example of typical results for a benthic incubation are shown in Fig. A1.2. Mussel metabolism results in the loss of dissolved oxygen and the excretion of dissolved phosphorus. Total dissolved phosphorus (TDP) includes both soluble reactive phosphorus (SRP; primarily inorganic), and dissolved organic phosphorus. While most of the P excreted by mussels is SRP, which is directly available for uptake by algae, a significant portion of excreted P may also be in the dissolved organic form. While this form of P is not directly available to algae, it can be made available either through microbial decomposition, or through hydrolysis by alkaline phosphatase, an extracellular enzyme released by many algae.

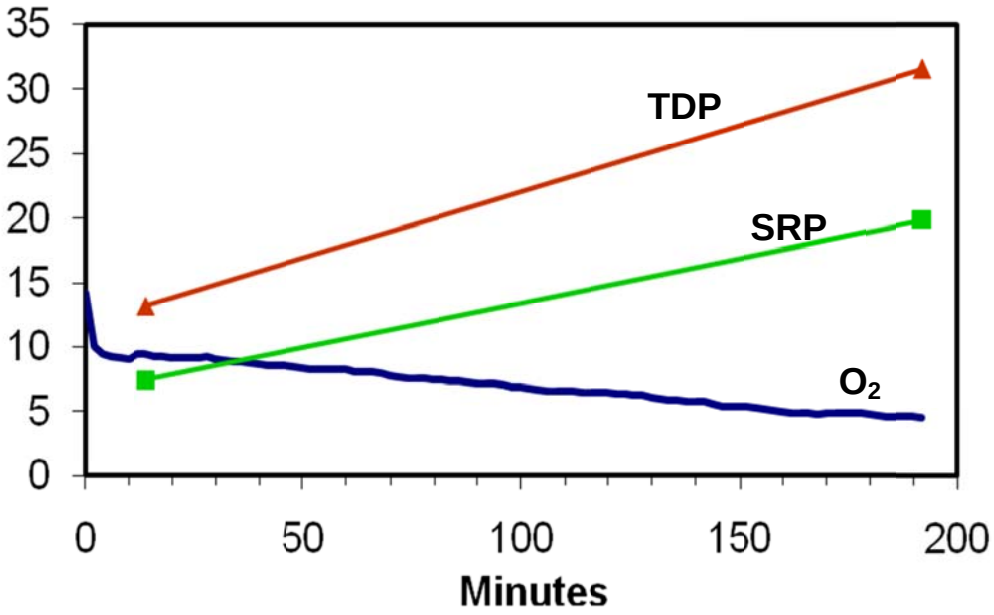

Fig. A1.2. Changes in dissolved oxygen, soluble reactive phosphorus (SRP), and total dissolved phosphorus (TDP) within a benthic chamber placed on rock over a mussel bed at the Green Can study site. Incubation surface area was 189 cm^2, and chamber volume was 1.45 liters.

To determine whether phosphorus excretion rates measured in chambers were due primarily to mussel metabolism (as opposed to other benthic invetebrates and bacteria), an experiment was conducted in which P excretion in benthic chambers was compared with P excretion by mussels placed in 60 ml syringes (Fig. A1.1). The results indicated that P excretion rates in the two chambers were equal when normalized to mussel biomass (measured as the dry weight of non-shell tissue) (Table A1.1). Therefore the excretion rates measured in benthic chambers can be attributed to quagga mussel metabolism.

Table A1.1. Comparison of P excretion rates normalized to quagga mussel biomass for chamber experiments and syringe experiments on Sep. 1, 2009. gDW = grams dry weight.

Incubation Type	SRP excretion (μg gDW hr^{-1})	TDP excretion (μg gDW hr^{-1})
Benthic Chamber	5.0	7.4
Syringe	5.0 ± 0.77	6.7 ± 0.94

A comparison of quagga mussel metabolic rates on five separate dates during the study period is given in Table A1.2. Respiration rates, as measured by oxygen consumption, were lowest on the first two dates, when water temperatures were cold, and increased with temperature on subsequent dates. The lowest P excretion rate was also observed on one of the cold days, but relatively high P excretion rates were observed on August 21, when water temperatures were also cold. The reason for the high rate on this date is unclear. Our previous lab experiments have highlighted the importance of temperature as a factor regulating P excretion by quagga mussels (Bootsma et al. 2008b). However, mussel density, mussel size, and food availability can also influence P excretion rates.

The influence of mussel metabolism on algal abundance in Lake Michigan can be explored by examining the carbon:phosphorus (C:P) ratio of various nutrient pools. Since phosphorus is the limiting nutrient for algae in Lake Michigan, the amount of phosphorus available to algae will determine the amount of carbon, or biomass, that the algae are able to produce. C:P ratios for various nutrient pools in Lake Michigan are listed in Table A1.3. The comparison indicates that mussels tend to release C and P at a ratio similar to that of the phytoplankton on which they feed. However, *Cladophora* tends to have a much higher C:P ratio, almost two times greater than that of phytoplankton. This reflects the ability of *Cladophora* to grow on very low concentrations of phosphorus. **As a result, the phosphorus that is excreted by mussels (which is derived primarily from the consumption of phytoplankton) can potentially lead to the production of *Cladophora* biomass that is twice as great as that of the phytoplankton from which the phosphorus originated**. Hence high *Cladophora* biomass results both from the accumulation of dissolved phosphorus in the near-bottom layer, due to mussel excretion, and from the ability of *Cladophora* to synthesize a large amount of biomass with a very small amount of phosphorus.

Table A1.2. Quagga mussel oxygen consumption rates and phosphorus excretion rates measured on five dates at the Green Can study site. The C:P ratio represents the amount of CO_2 respired relative to the amount of dissolved P excreted. Respired CO_2 was determined using the oxygen uptake rates and assuming a respiratory quotient of 1.0.

Date	Temp. (^oC)	O_2 uptake (mg m^{-2} hr^{-1})	SRP excretion (mg m^{-2} hr^{-1})	TDP excretion (mg m^{-2} hr^{-1})	C:P Molar ratio	Mussels (m^{-2})	Mussels gDW m^{-2}
8/21/09	5.3	32.0	0.240	0.313	99	23,228	145
8/27/09	7.5	21.3	0.074	0.145	143	21,623	93
9/1/09	15.2	132.1	0.376	0.555	231	15,634	75
9/4/09	16.6	*	0.264	0.573	150	8,505	92
9/10/09	16.1	182.0	0.320	0.395	446	23,159	155

* Dissolved oxygen probe did not function properly.

Table A1.3. C:P ratios of various biotic and abiotic nutrient pools in Lake Michigan. Phytoplankton and *Cladophora* C:P ratios are the ranges measured between 2006 and 2009. Mussel excretion C:P ratios are those measured in 2009. Molar units are used because they are most relevant to biological processes and they are less ambiguous than mass terms. Molar C:P ratios can be converted to mass C:P ratios by multiplying by 0.387.

Nutrient Pool	C:P Ratio (molar)
Phytoplankton	150 - 250
Mussel Excretion	99 – 446 (mean = 214)
Cladophora	300 - 450

Particle Image Velocimetry Measurements

The Particle Image Velocimetry (PIV) system used to measure particle flux rates above mussel beds is shown in Fig. A1.3. The system was deployed on several dates, with optimal results being obtained on September 1. (Data quality on other dates was compromised by technical problems, including high ambient light which saturates the digital images, and improper focusing of the camera). In Fig. A1.4, the results of PIV deployments over a mussel bed and over sediment with no mussels are shown. These plots clearly illustrate the effect of mussels on particle concentration in the near-bottom boundary layer. Over sediment with no mussels, there is an increase in particle concentration within a 2 to 4 cm thick layer immediately above the sediment, which is probably due to the accumulation of sinking particles and resuspension of bottom sediment. In contrast, the layer of water 4 to 6 cm above the mussel bed was depleted of particles, due to filtration by mussels.

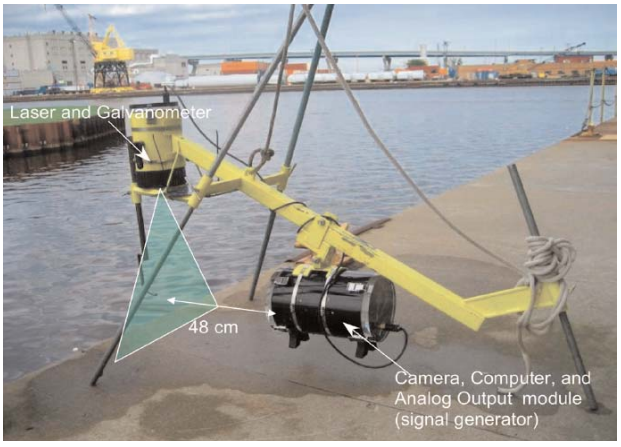

Fig. A1.3. The underwater Particle Image Velocimetry (PIV) system. Water motion is measured by using a high resolution camera to track natural particles in the water column, which are illuminated by a sweeping laser beam.

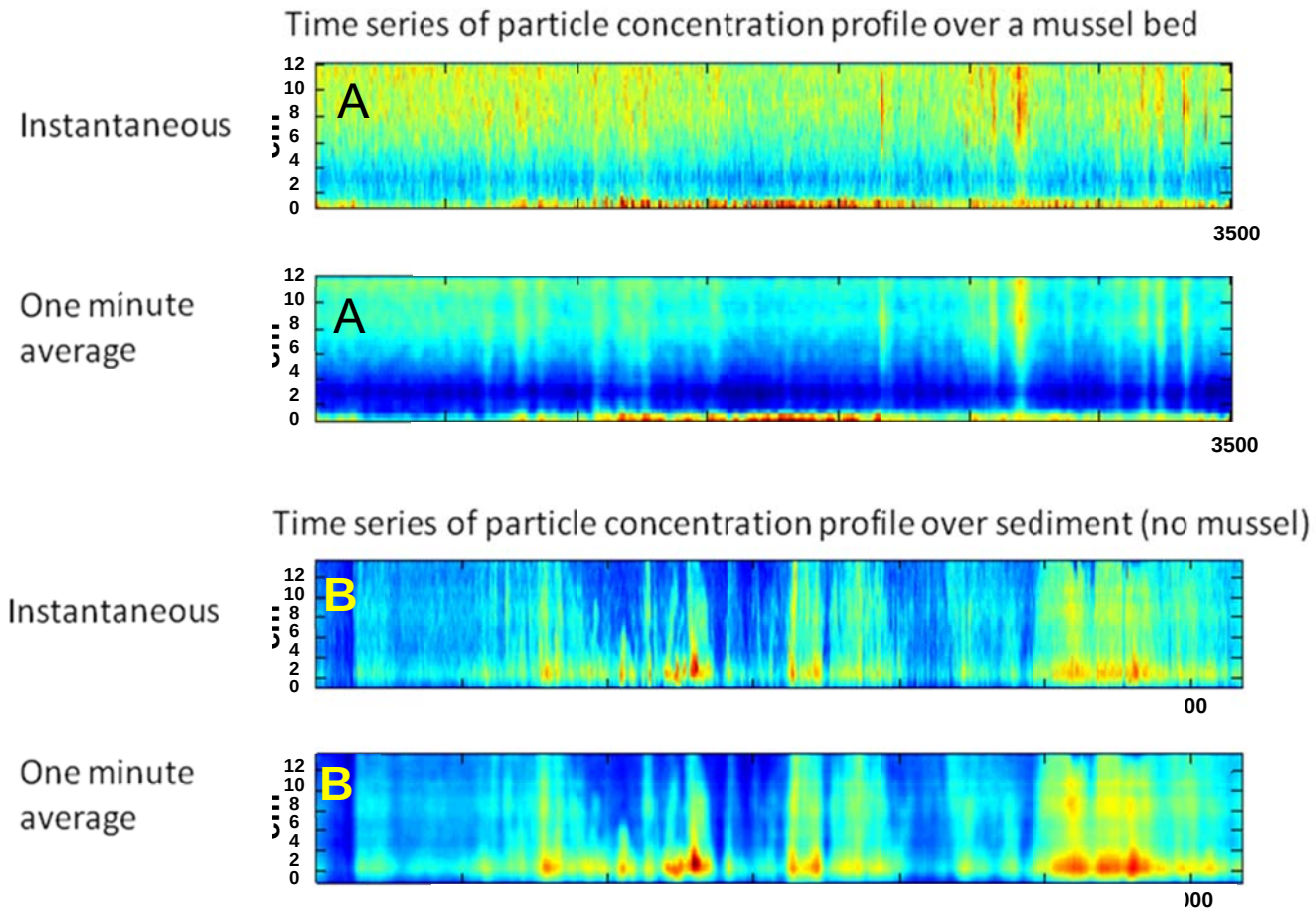

Fig. A1.4. Time series of particle concentration in the near-bottom water layer over a mussel bed (A), and over sediment with no mussels (B) at the Green Can study site. Colors represent the relative abundance of particles with dark blue being low and dark red being high. (Note that red and yellow areas at the bottoms of the plots for the mussel bed are artifacts due to mussels within this layer.)

Grazing Rates, Clearance Rates, and Dissolved Phosphorus Excretion

Particle concentration profiles (Fig. A1.4) can be used along with turbulent flux profiles (Fig. A1.5) to calculate mussel grazing and cleareance rates[1]. Grazing rate can be determined using the following method: Considering a water column with a unit cross-sectional area above the mussel bed with height = *z*, the mass balance of particles in the column can be given as:

[1] Grazing rate is the number or mass of particles consumed per unit time, while clearance rate is the volume of water that is completely cleared of particulate material per unit time.

$$\frac{d\left(\int_0^z C(z',t)dz'\right)}{dt} = -\overline{w'c'} - WC + G \qquad \text{(A1.1)}$$

$C(z, t)$ = the linear regression of the ensemble mean particle concentration or a low-pass filtered concentration

c' = $c(z,t) - C(z,t)$, the deviation of the instantaneous concentration from the linearly growing mean

w = vertical velocity

$\overline{-w'c'}$ = the measured vertical turbulent flux of particles (i.e., the cross-correlation of fluctuating velocity and particle concentration)

W = the averaged vertical velocity (settling speed); thus $-WC$ accounts for the mass increase due to settling

G = source/sink term that characterizes the combined effect of mussel grazing and particle resuspension

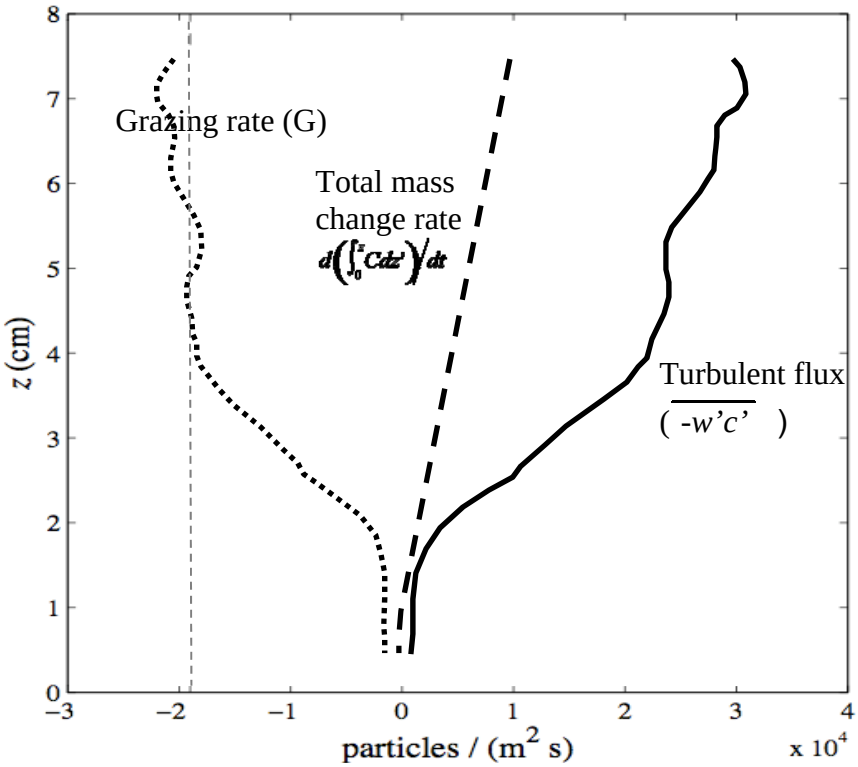

Figure A1.5. A sample result shows the measured profiles of terms in equation (A1.1), neglecting the settling term –*WC*. Total areal grazing rate is represented by the gray vertical dashed line.

With measurements of the mass change rate, turbulent flux and settling rate, the grazing rate *G* can be calculated through this equation. In the nearshore zone shallow water with strong hydrodynamic forcing, the settling term was found to be negligible compared with the turbulent flux, while in the offshore zone hypolimnion during the stratified season, settling could be the limiting transport term of the mass balance. The validity of equation (A3.1) can be justified if the calculated profile of $G(z)$ reaches a constant value over a short distance above the boundary (see Fig. A1.5).

The grazing rate can also be modeled as

$$G = QC_0 \tag{A1.2}$$

where C_0 is the near-bed plankton concentration and Q is the water pumping rate in terms of volume per unit area per unit time. Our detailed measurement with the PIV revealed that a strong concentration gradient exists immediately above the mussel colony (Fig. A1.4). The thickness of this layer is controlled by the strength of hydrodynamic condition, and it usually increases when mixing decreases, reaching a maximum of about 5 cm with a dense mussel population. With the measurement of the nearbed concentration within the particle "depleted" layer, C_0, the mussels' pumping rate can be determined as

$$Q_p = \frac{G}{C_0 D} \tag{A1.3}$$

where D is the density of mussels (individual per m^2). Using a mussel density of 10,000 m^{-2} and the PIV data obtained at the Green Can site, the estimated mussel pump rate is 3.9 liter per day per mussel. This is higher than the rate previously assumed when estimating mussel feeding capacity in Lake Michigan (~1 liter per mussel per day), but it is within the range of values reported for previous laboratory studies (Baldwin et al. 2002).

A similar approach can be used to estimate the upward flux of dissolved phosphorus from mussel beds, if the vertical distribution of dissolved phosphorus and the near-bed distribution of the turbulent diffusivity are known. For the nearshore bottom, if hydrodynamic mixing is sufficiently high, a log-law[2] may be applied to the observed current profile, and the turbulent diffusivity (or equivalently turbulent viscosity) can be modeled as

$$D_T = \kappa u_* z \tag{A1.4}$$

where

κ = von Karmen's constant[3] (0.41)

[2] The current velocity at any distance above the lake bottom is proportional to the log of that distance.
[3] Describes the logarithmic water velocity profile created by shear stress near a boundary.

μ_* = shear velocity
z = height above the lake bottom.

A logarithmic profile for $C - C_0$ would be expected, where C_0 is the SRP concentration near the bottom if the bottom is the net source of SRP. This is verified by a measured microprofile (Fig. A1.6). Therefore the Reynolds analogy[4] can be applied to estimate the flux of SRP (F) following:

$$C_0 - C(z) = \frac{F}{-\kappa u_*} \ln z \qquad \text{(A1.5)}$$

For the case presented in Fig. A1.6, F = 16.3 mg m^2 day^{-1} (0.69 mg m^{-2} hr^{-1}). This is about two times greater than the values reported in Table A1.2. The difference may in part be an artifact due to the different methods (e.g. placement of benthic chambers may temporarily disturb mussels and result in lower P excretion rates), but it may also be real, since the SRP profile measurements and the chamber incubations were conducted on different dates. *In situ* P excretion rates measured on multiple dates in previous years (Bootsma et al. 2008a; Bootsma 2009) were usually between 0.2 and 0.8 mg m^{-2} hr^{-1}, and the PIV-derived rate of 0.69 mg m^{-2} hr^{-1} is within this range. The advantage of the PIV / micro-profile approach is that it may allow us to explore the effect of flow conditions on dissolved P flux, which is not possible within chambers that hinder flow. Flow conditions will determine the extent to which *Cladophora* may utilize dissolved P released by mussels. Under low flow (low turbulence) conditions, *Cladophora* may be able to assimilate most of the dissolved P excreted by mussels, but under high flow (high turbulence) conditions, dissolved P excreted by mussels will rapidly diffuse into the overlying water column, with little being assimilated by *Cladophora*. Future use of the PIV approach demonstrated here will allow us to directly measure the influence of turbulence on the mussel – *Cladophora* phosphorus link, and to use this relationship to more directly link the existing mussel and *Cladophora* models.

The PIV-derived phosphorus excretion rate presented here suggests that the role of dreissenid mussels as a source of dissolved phosphorus in the Lake Michigan nearshore zone surrounding Milwaukee is as great as, or greater than, that previously estimated (Bootsma et al. 2008a). If this rate is applied to a 10 meter water column in which there is no loss of SRP to algal uptake or offshore mixing, it would result in a daily increase in the water column SRP concentration of about 1 μg L^{-1}. SRP concentration within the nearshore zone is usually less than 1 μg L^{-1}, indicating that the excreted SRP is lost to algal uptake and/or offshore mixing. However, offshore SRP and total P concentrations have been decreasing (Mida et al. 2010), suggesting that little of the SRP generated by mussels in the nearshore zone is lost to the offshore zone. The conclusion is

[4] The Reynolds analogy assumes that mass (e.g. SRP) flux is equal to turbulent momentum flux.

that much of the SRP excreted by mussels is assimilated by nearshore algae, of which *Cladophora* is by far the dominant component. In addition, considering that quagga mussels are a more important source of SRP in the nearshore zone than is direct river loading (with the exception of regions in immediate proximity to river mouths), it is highly unlikely that *Cladophora* biomass would be as great as that currenly observed if dreissenid mussels were not present.

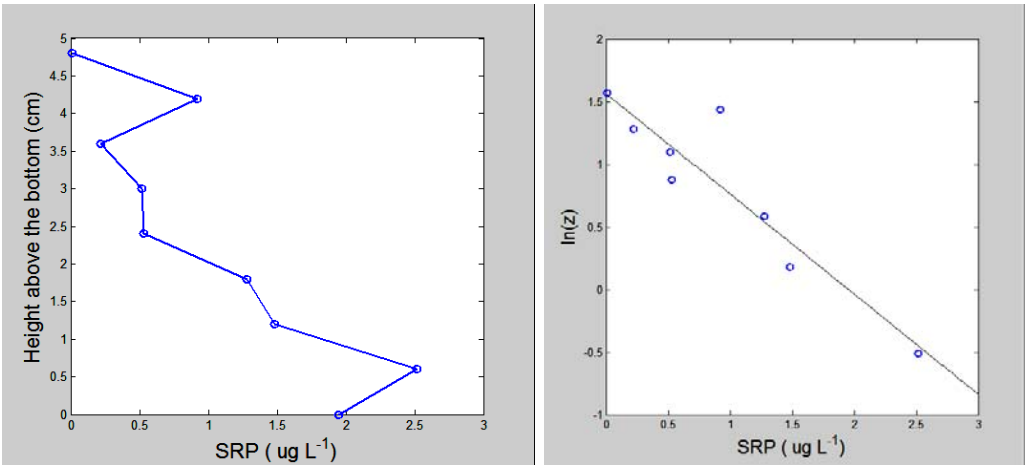

Fig. A1.6. Vertical profile of soluble reactive phosphorus (SRP) in the near-bottom layer, immediately above a quagga mussel bed. The upward flux of SRP is determined using equation A1.5, where C_0-C(z) is the vertical SRP gradient shown in the above plots.

Appendix II. Identifying Major Phosphorus Pathways in the Lake Michigan Nearshore Zone with $^{90}Y/^{90}Sr$ and $^{234}Th/^{238}U$ Radionuclide Tracers

Introduction

In the nearshore zone of Lake Michigan, a large fraction of the total phosphorus pool is associated with particles. The fate of this particulate phosphorus has a strong influence on biological processes, especially algal production, within the nearshore zone. For example, if this phosphorus remains in particulate form, it may eventually be transported to the offshore zone and become permanently buried in deeper parts of the lake. However, if it is consumed by quagga mussels, it may be converted to mussel biomass, or it may be released in a dissolved form that is available to algae, including *Cladophora*. Particulate phosphorus released by mussels in the form of feces or pseudofeces may also support the growth of a microbial community (bacteria and protozoans), which, like mussels, may metabolize phosphorus and release it in dissolved form.

Determining the fate of particles in the nearshore zone using conventional methods, such as sediment traps and benthic incubators, is difficult due to processes such as particle resuspension and heterogeneous distribution on the lake bottom. To circumvent these problems, a novel method that measures nearshore particle and nutrient cycling using naturally occurring $^{90}Y/^{90}SR$ and $^{234}Th/^{238}U$ radionuclide tracers has been applied.

$^{234}Th/^{238}U$ activity ratios have been utilized for decades in marine and freshwater systems as a tracer for particle flux – where disequilibrium between particle-reactive ^{234}Th (half-life: 24.1 days) and its conservative parent ^{238}U measures particle removal rates on a time scale of days to weeks. A new tracer that has been developed utilizes $^{90}Y/^{90}Sr$ activity ratios – where disequilibrium between particle-reactive ^{90}Y (half-life: 64 hours) and its conservative parent ^{90}Sr measures particle removal rates on a time scale of hours to days. When both tracers ($^{90}Y/^{90}Sr$ & $^{234}Th/^{238}U$) are used in tandem, net particle removal rates on both time scales are measured.

The goal of this portion of the study was to measure the flux of mass and particulate phosphorus from the water column to the lakebed in the nearshore zone of Lake Michigan using the radionuclide tracers mentioned previously.

Methods

Sample collection: Water samples (~50 L) were collected five times (August 20, 25, 28, 31 and September 10, 2009) at a shallow (20 meter) site in southern Lake Michigan (See Fig. 1, page 9). Samples for total suspended matter, nutrients and radionuclide measurements were collected from 3 m, 10 m and 17

m depths using a submersible pump. Lake bottom flocculent and dreissenid mussel ejecta were collected by the Bootsma Laboratory.

Chemistry: The methodology for all radionuclide measurements is described in Waples and Orlandini (2011) and Waples et al. (2003). All nutrient analyses are described in Standard Methods. Propagated errors on all activity measurements presented here represent ±1 standard deviation.

Ancillary data: An instrumented (PIONEER) mooring was deployed at the Green Can sampling site over the duration of the sampling period. Sondes (YSI) located 1 meter below the surface and ~1 meter above the bottom recorded turbidity, chlorophyll and other standard parameters. Water currents (3-D) were measured for the duration of the experiment with a bottom mounted (upward-looking) SonTek acoustic Doppler current profiler (ADCP. 1000 kHz; averaging interval: 60s, profiling interval: 600s).). "Gross" particle fluxes were measured with a McLane sequencing sediment trap deployed at a depth of 10m (mid water column depth). A total of 21 samples were collected with discrete samples collected every 24 hours.

Theory

Radionuclide flux: In a one-box model (see Savoye et al. 2006), the temporal change in ^{234}Th activity ($\partial A_{Th} / \partial t$) is expressed as:

$$\frac{\partial A_{Th}}{\partial t} = \lambda_{Th}(A_U - A_{Th}) - P_{Th} + V_{Th} \qquad \text{(A2.1)}$$

where the total activities of ^{238}U (A_U) and ^{234}Th (A_{Th}) integrated over the depth of the water column are expressed in dpm m^{-2}, the decay constant for ^{234}Th (λ_{Th}) is equal to 0.02876 d^{-1}, the net downward removal flux of ^{234}Th (P_{Th}) is expressed in dpm m^{-2} d^{-1}, and V_{Th} is equal to the sum of horizontal advective and diffusive fluxes of ^{234}Th normalized to horizontal surface area, expressed as dpm m^{-2} d^{-1}. Similarly, the temporal change in ^{90}Y activity ($\partial A_Y / \partial t$) is expressed as:

$$\frac{\partial A_Y}{\partial t} = \lambda_Y(A_{Sr} - A_Y) - P_Y + V_Y \qquad \text{(A2.2)}$$

where the total depth integrated activities of ^{90}Sr (A_{Sr}) and ^{90}Y (A_Y) are expressed in dpm m^{-2}, the decay constant for ^{90}Y (λ_Y) is equal to 0.25993 d^{-1}, the net downward removal flux of ^{90}Y (P_Y) is expressed in dpm m^{-2} d^{-1}, and V_Y is equal to the sum of horizontal advective and diffusive fluxes of ^{90}Y.

Under steady-state conditions, which are initially assumed for the sake of clarity, the change in inventories of total ^{234}Th and ^{90}Y remains constant over time, such that $\partial A_{Th} / \partial t$ and $\partial A_Y / \partial t$ are equal to zero. If it is also assumed that the sum of

horizontal advective and diffusive fluxes (V_{Th} and V_Y) is negligible, then the net downward flux of ^{234}Th (P_{Th}) and ^{90}Y (P_Y) can be expressed as:

$$P_{Th} = \lambda_{Th}(A_U - A_{Th}) \quad \text{(A2.3)}$$

and

$$P_Y = \lambda_Y(A_{Sr} - A_Y) \quad \text{(A2.4)}$$

If, however, the inventories of total ^{234}Th and ^{90}Y change over time, then non steady-state solutions for $P_{(Th)}$ and $P_{(Y)}$ can be expressed as:

$$P_{Th} = \lambda_{Th}\left[\frac{A_U(1-e^{-\lambda_{Th}\Delta t}) + A_{Th1}e^{-\lambda_{Th}\Delta t} - A_{Th2}}{1-e^{-\lambda_{Th}\Delta t}}\right] \quad \text{(A2.5)}$$

and

$$P_Y = \lambda_Y\left[\frac{A_{Sr}(1-e^{-\lambda_Y\Delta t}) + A_{Y1}e^{-\lambda_Y\Delta t} - A_{Y2}}{1-e^{-\lambda_Y\Delta t}}\right] \quad \text{(A2.6)}$$

where A_1 and A_2 represent the total areal water column inventories of ^{234}Th and ^{90}Y for the first (initial) and second (subsequent) sampling periods, respectively, and the sum of horizontal advective and diffusive fluxes (V_{Th} and V_Y) is still assumed to be negligible.

Mass and particulate phosphorus flux: If the ratio of mass to ^{234}Th and ^{90}Y activity on particles is known (i.e., $mass / A_{Th}^P$ and $mass / A_Y^P$; expressed as g dpm^{-1}), then the net downward flux of mass can be expressed using both the ^{234}Th and ^{90}Y tracer as:

$$P_{mass(Th)} = P_{Th} \times \frac{mass}{A_{Th}^P} \quad \text{(A2.7)}$$

and

$$P_{mass(Y)} = P_Y \times \frac{mass}{A_Y^P} \quad \text{(A2.8)}$$

where $P_{mass(Th)}$ and $P_{mass(Y)}$ are expressions of net mass flux relative to each radionuclide tracer. The net downward flux of particulate phosphorus (i.e., $P_{PP(Th)}$ and $P_{PP(Y)}$) can similarly be calculated simply by replacing the ratio of mass to ^{234}Th and ^{90}Y activity on particles with the ratio of particulate phosphorus (PP) to

^{234}Th and ^{90}Y activity on particles (i.e., PP / A_{Th}^{P} and PP / A_{Y}^{P}; expressed as mg dpm^{-1}).

$$P_{PP(Th)} = P_{Th} \times \frac{PP}{A_{Th}^{P}} \quad \text{(A2.9)}$$

$$P_{PP(Y)} = P_{Y} \times \frac{PP}{A_{Y}^{P}} \quad \text{(A2.10)}$$

Results and Discussion

Radionuclide, total suspended matter and particulate phosphorus inventories: Water column measurements of both particulate (> 0.45 um, ^{234}Th^{part}, ^{90}Y^{part}) and dissolved (< 0.45 um, ^{234}Th^{diss}, ^{90}Y^{diss}) radionuclide activities, total suspended matter (TSM) concentrations, and particulate phosphorus (PP) concentrations are presented in Table A2.1.

Table A2.1. Nearshore zone ^{234}Th and ^{90}Y activity measurements at station "Green Can" in southern Lake Michigan. TSM = total suspended matter; PP = particulate phosphorus; A^{part} = activity of ^{234}Th and ^{90}Y on particulate matter > 0.45 μm; A^{diss} = activity of ^{234}Th and ^{90}Y in the dissolved phase < 0.45 μm.

Collected	Depth m	TSM g m^{-3}	PP mg m^{-3}	^{234}Th^{part} dpm m^{-3}	^{234}Th^{diss} dpm m^{-3}	^{90}Y^{part} dpm m^{-3}	^{90}Y^{diss} dpm m^{-3}
20 Aug 2009	3	1.0	1.9	86 ± 1	62 ± 1	37 ± 7	437 ± 17
	10	0.5	2.1	207 ± 2	63 ± 1	45 ± 7	539 ± 18
	17	0.8	1.7	63 ± 1	110 ± 1	28 ± 10	518 ± 17
25 Aug 2009	3	1.3	2.9	61 ± 1	38 ± 1	69 ± 9	357 ± 8
	10	0.6	2.6	101 ± 2	89 ± 1	19 ± 9	398 ± 14
	17	0.5	2.0	78 ± 1	91 ± 1	28 ± 5	398 ± 20
28 Aug 2009	3	0.6	2.4	161 ± 2	56 ± 1	36 ± 4	569 ± 15
	10	0.7	4.4	126 ± 2	63 ± 1	32 ± 7	497 ± 12
	17	0.6	2.7	103 ± 1	66 ± 1	19 ± 7	645 ± 29
31 Aug 2009	3	0.7	2.4	71 ± 1	49 ± 1	48 ± 6	490 ± 12
	10	0.6	2.4	92 ± 1	45 ± 1	44 ± 10	415 ± 20
	17	1.0	2.7	47 ± 1	36 ± 1	39 ± 6	328 ± 10
10 Sep 2009	3	0.5	2.3	109 ± 1	67 ± 1	19 ± 8	587 ± 29
	17	0.8	3.1	56 ± 1	43 ± 1	33 ± 4	382 ± 18

Areal integrated (trapezoidal) 0-20 meter water column inventories of total ^{234}Th and total ^{90}Y (i.e., dpm m^{-2}) over the five sampling dates are shown in Fig. A2.1. Total radionuclide activities were calculated as the sum of both dissolved and particulate fractions. Radionuclide activities at 0 and 20 meters depth were assumed to equal those measured at 3 and 17 meters depth, respectively. A ^{238}U activity of 230 ± 20 dpm m^{-3} was based on previous measurements (Waples et al. 2003). A ^{90}Sr activity of 759 ± 18 dpm m^{-3} was measured at the 'Green Can' site (3 meters depth) on 28 August 2009. Both parent radionuclide activities (and inventories) were assumed to remain constant over the course of the sampling period.

Radionuclide flux: The net downward flux of both ^{234}Th (P_{Th}) and ^{90}Y (P_Y) were calculated using the integrated (trapezoidal) 0-20 meter inventories of total ^{234}Th and total ^{90}Y and non-steady-state equations 5 and 6 (Fig. A2.2). ^{90}Y fluxes ranged from a high of 2209 ± 177 dpm m^{-2} d^{-1} on August 31 to a low of 73 ± 201 dpm m^{-2} d^{-1} on August 28. ^{234}Th fluxes ranged from a high of 560 ± 15 dpm m^{-2} d^{-1} on August 31 to a low of -217 ± 17 dpm m^{-2} d^{-1} on August 28. The negative thorium flux on August 28 is due to the relatively sharp increase in areal ^{234}Th activity that occurred between August 25 and August 28 (see Fig. A2.1). Non-steady-state conditions were chosen because the conditions for steady-state (i.e., $\partial A_{Th} / \partial t$ and $\partial A_Y / \partial t$ are equal to zero) did not hold true. In Fig. A2.1, inventories of ^{234}Th varied ~20% to ~80% between sampling periods, while inventories of ^{90}Y varied ~10 to ~30%.

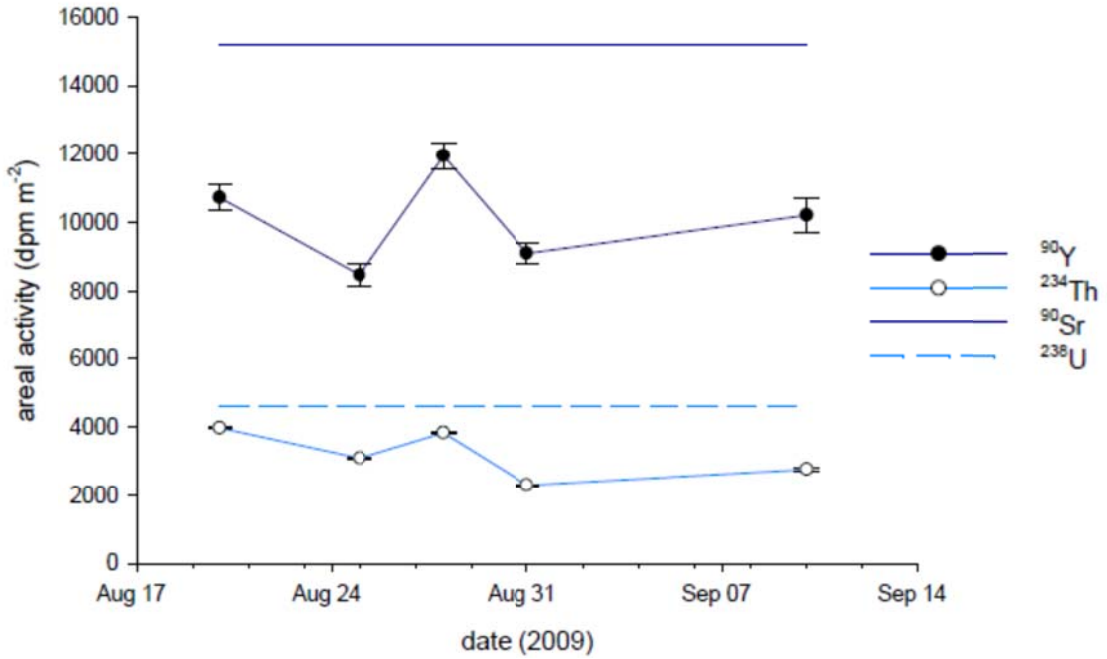

Fig. A2.1. Water column (0 – 20 meters) integrated areal activities of total ^{234}Th (open circles) and total ^{90}Y (filled circles) as a function of time.

Mass flux: Estimates of the net downward flux of suspended material (i.e., $P_{mass(Th)}$ and $P_{mass(Y)}$) were calculated with non steady-state radionuclide fluxes (P_{Th} and P_Y) and measured mass/activity ratios (at 17 meters depth) using equations 7 and 8. Calculated net mass fluxes (shown in Table A2.2) that were derived from $^{234}Th/^{238}U$ disequilibrium measurements ranged from a high of 7.9 ± 0.3 g m^{-2} d^{-1} on August 31 to a low of -1.4 ± 0.1 g m^{-2} d^{-1} on August 28 (where negative fluxes indicate an injection of material to the water column). Calculated net mass fluxes that were derived from $^{90}Y/^{90}Sr$ disequilibrium measurements ranged from a high of 68 ± 27 g m^{-2} d^{-1} on August 31 to a low of 2 ± 5 g m^{-2} d^{-1} on August 28.

With the exception of August 28, differences in ^{234}Th-derived versus ^{90}Y-derived flux estimates were large. Average fluxes (between August 25 and September 10) were generally an order of magnitude lower with the ^{234}Th tracer than with the ^{90}Y tracer. An explanation for this discrepancy is discussed below.

Particulate phosphorus flux: Estimates of the net downward flux of suspended material (i.e., $P_{PP(Th)}$ and $P_{PP(Y)}$) were calculated with non steady-state radionuclide fluxes (P_{Th} and P_Y) and measured PP/activity ratios (at 17 meters depth) using equations A2.9 and A2.10. Calculated particulate phosphorus fluxes from the water column to the lakebed (shown in Table 2) that were derived from $^{234}Th/^{238}U$ disequilibrium measurements ranged from a high of 23.5 ± 0.8 mg m^{-2} d^{-1} on August 31 to a low of -5.6 ± 0.5 mg m^{-2} d^{-1} on August 28 (where negative fluxes indicate an injection of particulate phosphorus to the water column). Calculated fluxes of particulate phosphorus that were derived from $^{90}Y/^{90}Sr$ disequilibrium measurements ranged from a high of 235 ± 94 mg m^{-2} d^{-1} on August 31 to a low of 8 ± 22 mg m^{-2} d^{-1} on August 28.

Table A2.1 – Fluxes of total suspended matter (TSM) and particulate phosphorus (PP) as determined by the non steady-state measurements of ^{234}Th and ^{90}Y flux and the measured concentration/activity ratios of TSM and PP and ^{234}Th and ^{90}Y at depth (17 meters).

Collected	TSM g m^{-3}	PP mg m^{-3}	^{234}Th derived mass flux g m^{-2} d^{-1}	^{90}Y derived mass flux g m^{-2} d^{-1}	^{234}Th derived PP flux mg m^{-2} d^{-1}	^{90}Y derived PP flux mg m^{-2} d^{-1}
20 Aug 2009	0.8	1.7				
25 Aug 2009	0.5	2.0	2.0 ± 0.1	45 ± 18	5.5 ± 0.3	130 ± 51
28 Aug 2009	0.6	2.7	-1.4 ± 0.1	2 ± 5	-5.6 ± 0.5	8 ± 22
31 Aug 2009	1.0	2.7	7.9 ± 0.3	68 ± 27	23.5 ± 0.8	235 ± 94
10 Sep 2009	0.8	3.1	0.2 ± 0.1	32 ± 7	0.7 ± 0.2	104 ± 24

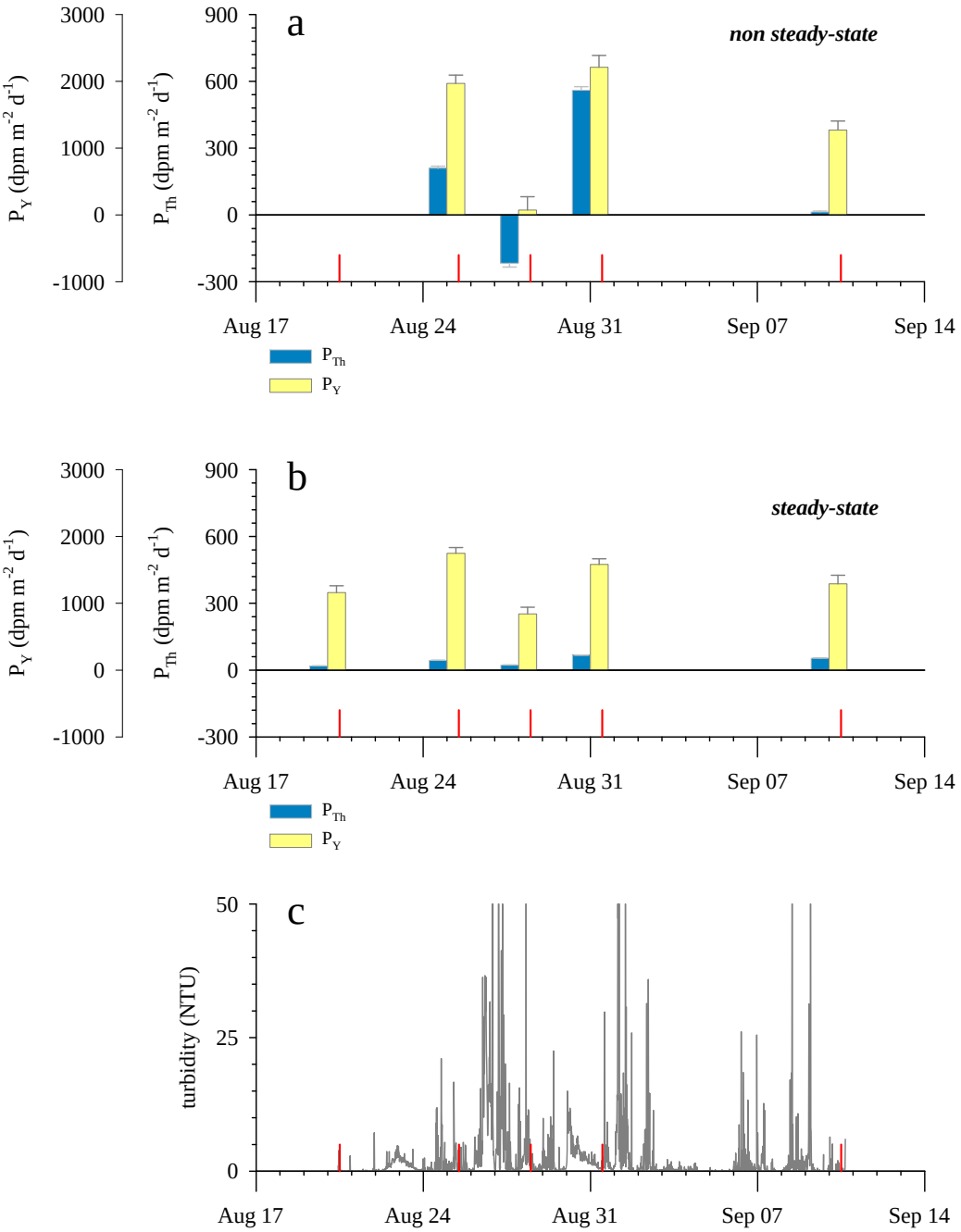

Fig. A2.2. (a) Non steady-state fluxes of ^{234}Th (blue) and ^{90}Y (yellow) from the water column. (b) Steady-state fluxes of ^{234}Th and ^{90}Y from the water column. Note difference in scale between ^{234}Th and ^{90}Y fluxes. Similarity between non steady-state and steady-state ^{90}Y fluxes indicates near steady-state conditions. ^{90}Y responds to changes much more quickly than ^{234}Th due to its shorter half-life. (c) Bottom turbidity measured with a YSI sonde. Vertical red lines indicate sampling dates.

With the exception of August 28, differences in ^{234}Th-derived versus ^{90}Y-derived flux estimates were again large – with ^{90}Y-derived fluxes of particulate phosphorus averaging much higher than their ^{234}Th-derived counterparts.

A comparison of mass fluxes at 10 meters depth: To address why flux estimates based on two different radionuclide tracers differed so much, radionuclide derived flux estimates can be compared with flux measurements that were made with a sediment trap. Because the surface opening of the trap was located at 10 meters depth, radionuclide derived flux estimates must also be adjusted or recalculated to reflect a material flux through the 10-meter deep plane. To do this, parent-daughter radionuclide inventories were recalculated on an areal basis from the surface to a depth of 10 meters, with mass/activity ratios measured at 10 meters depth used to convert flux measurements of dpm m^{-2} d^{-1} to g m^{-2} d^{-1}.

Looking at the sediment trap results first, Fig. A2.3 shows fairly uniform and small fluxes of material (median flux = 0.04 g m^{-2} d^{-1}) over the course of the sampling period (August 20 to September 9). The relatively large flux of material on August 29 (i.e., 1.94 g m^{-2} d^{-1}) can most likely be explained as a hydrodynamic (oversampling) artifact caused by strong currents that were present at the time (Fig. A2.4 and Fig. A2.5).

If the sediment trap flux measurements are then compared with the estimates of ^{234}Th and ^{90}Y-derived mass flux at the 10 meter deep plane (Fig. A2.6), it is apparent that while ^{234}Th-derived and sediment trap derived mass fluxes are generally of the same scale, ^{90}Y-derived mass fluxes are again much higher than the other two.

Based on Fig. A2.6, it would be easy to assume that the ^{90}Y-derived fluxes are unreasonable. However, the following solution is proposed:

i. The sediment trap fluxes are only measuring the flux of particles removed by gravitational settling (and any artifact introduced by the hydrodynamics of particle movement past the open trap mouth). In a circulating environment, the sediment trap will *not* measure particle removal due to physical *interception* (e.g., particle uptake by dreissenid mussels on the lakebed). The radionuclide tracers, on the other hand, *will*. Any means of radionuclide removal from the water column is registered in the measured parent/daughter disequilibrium. In a steady-state system, therefore, with active uptake of material along the lake bottom, sediment trap derived mass fluxes should be consistently lower than mass fluxes derived with either the ^{234}Th or ^{90}Y tracers.

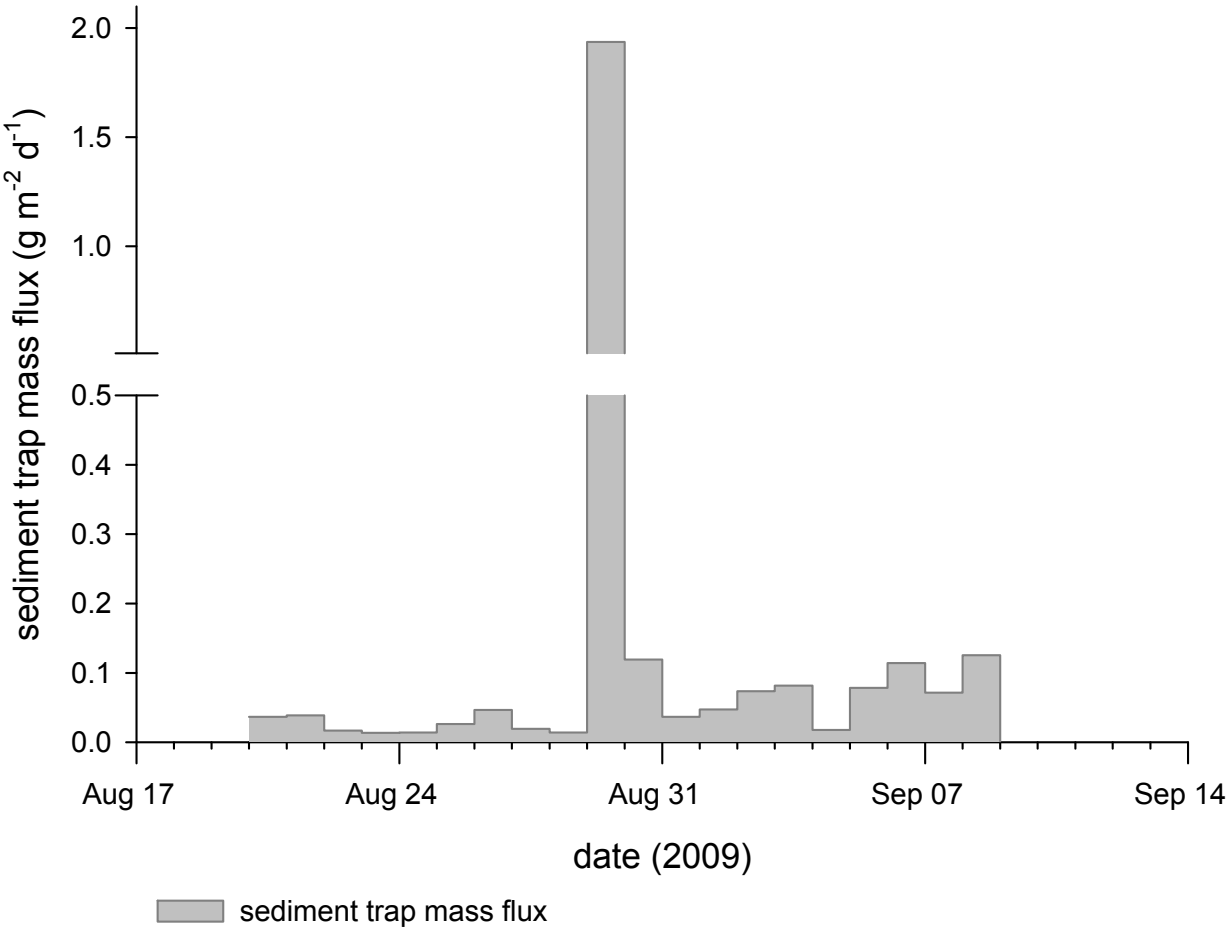

Fig. A2.3. Daily measurements of mass flux as measured by a sediment trap at 10 meters depth at 'Green Can' station.

ii. The discrepancy between ^{234}Th-derived mass fluxes and ^{90}Y-derived mass fluxes is explained in Waples and Orlandini (2010). Briefly, in a nearshore system with *no* sediment resuspension, both ^{234}Th and ^{90}Y-derived mass fluxes should be equal to each other. On the timeframe of the ^{234}Th tracer (halflife = 24.1 days), these conditions are essentially nonexistent in the nearshore zone of Lake Michigan. Sediment resuspension is occurring (nearly) constantly. When particles fall to the bottom and reside there for some time before being resuspended again, the ^{90}Y will decay much more rapidly than ^{234}Th (Fig. A2.7). Apparent disequilibrium (and resultant fluxes) will therefore appear larger for ^{90}Y (or smaller for ^{234}Th).

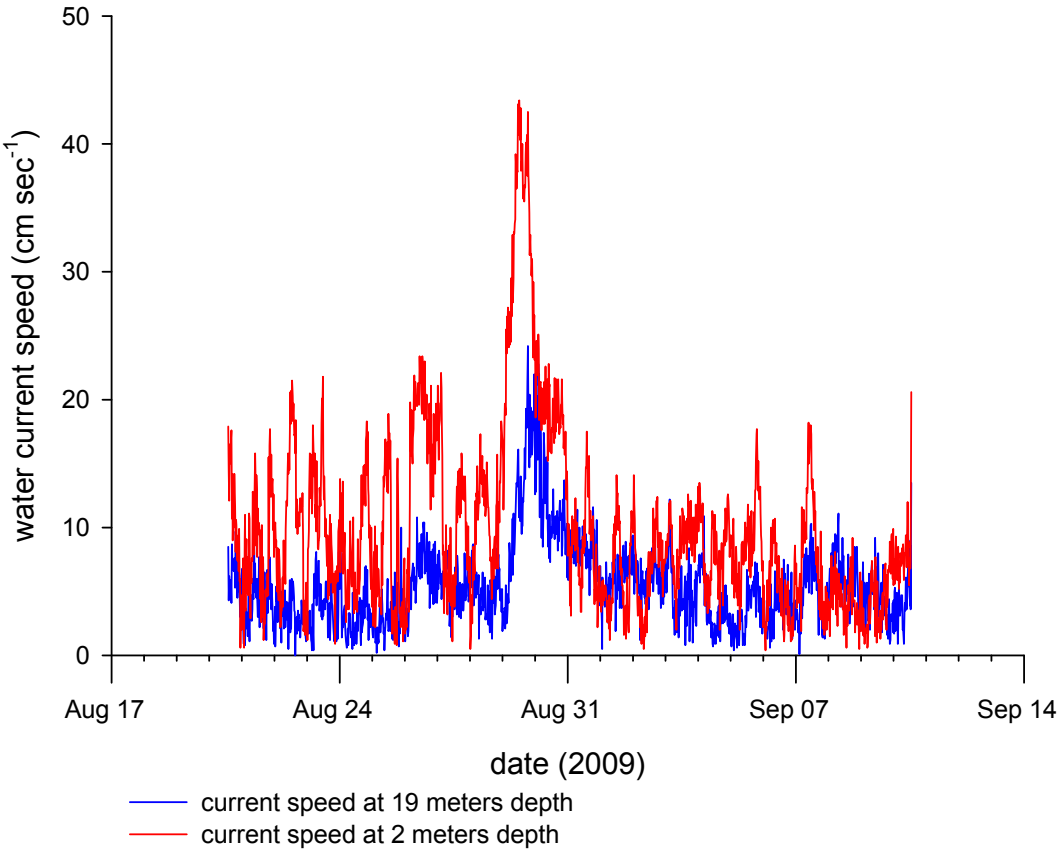

Fig. A2.4. Surface (red line) and bottom (blue line) water current speed at 'Green Can" station measured with a bottom mounted SonTek ADCP.

iii. It is important to understand that both ^{234}Th and ^{90}Y-derived flux estimates are "correct". Both tracers accurately measure net particle removal on timescales related to their half-lives. The ^{90}Y tracer is measuring particle net removal on a timescale of hours to days. The ^{234}Th tracer is measuring net particle removal on a timescale of days to weeks.

iv. Therefore, it is proposed that the ^{90}Y tracer is accurately measuring short term net particle removal at the 'Green Can' station. Further, it is proposed that the ^{234}Th tracer is measuring (on average) the offshore transport of material – or the flux of material to the offshore zone where permanent burial of sediment occurs. This is discussed extensively in Waples et al. (2004).

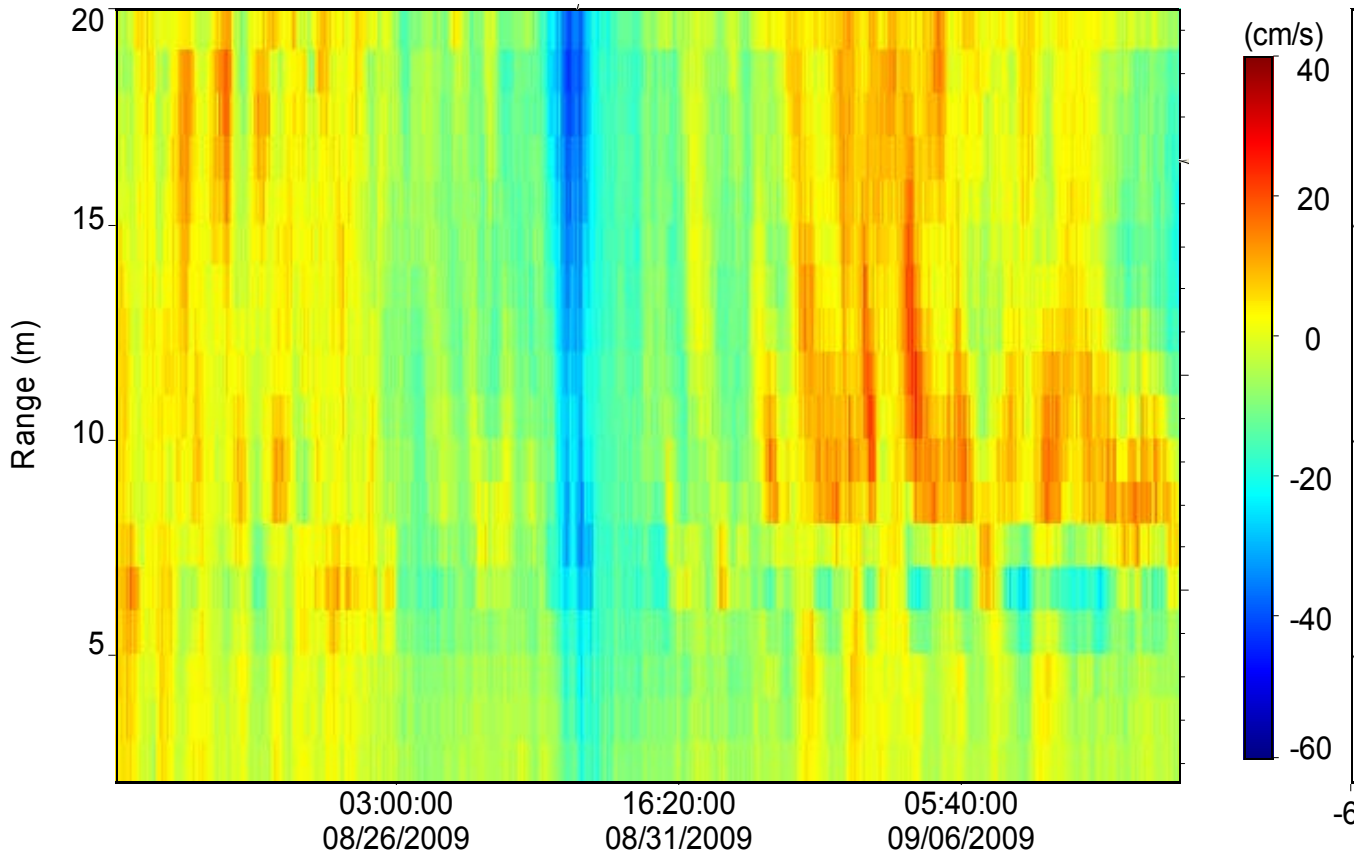

Fig. A2.5. Northerly component of water current velocity at 'Green Can' station measured with a bottom mounted (upward looking) SonTek ADCP. Velocities indicate the direction water is moving toward. Range is distance from current meter looking up toward surface.

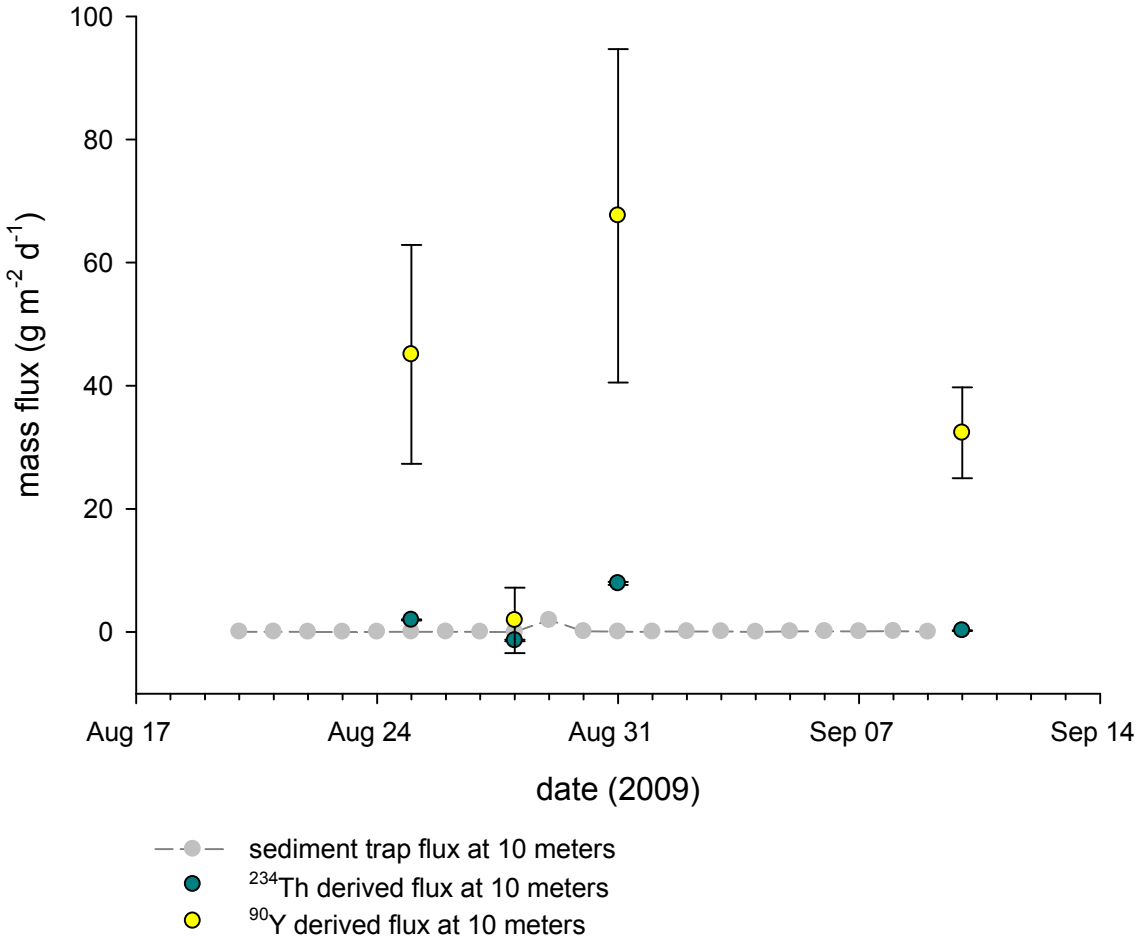

Fig. A2.6. A comparison of mass fluxes derived by sediment trap and ^{234}Th and ^{90}Y tracers at mid-water column depth at 'Green Can' station in southwestern Lake Michigan.

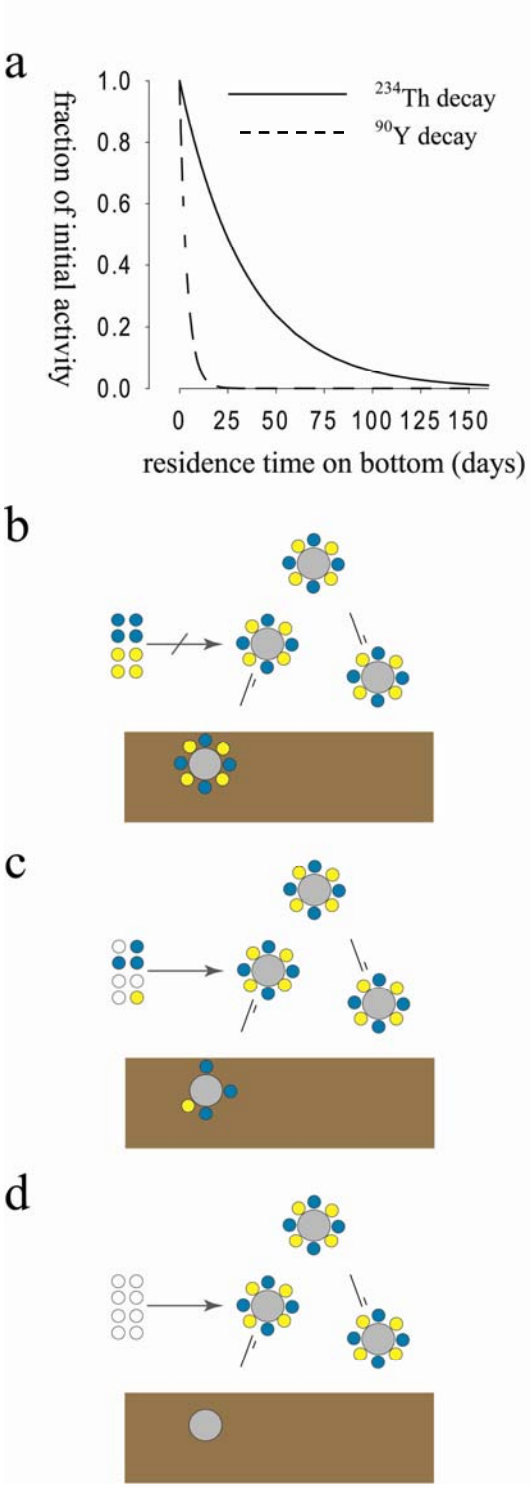

Fig. A2.7. (a) Activity of ^{234}Th and ^{90}Y on particles as a function of residence time on the bottom (*tb*). (b) Instantaneous resuspension (e.g., *tb* = minutes). (c) Intermediate interval resuspension (e.g., *tb* = days). (d) Long interval resuspension (e.g., *tb* = months). Yellow = ^{90}Y; Blue = ^{234}Th.

Dreissenid mussel clearance rates: There are several ways in which the validity of mass fluxes derived from $^{90}Y/^{90}Sr$ disequilibria can be examined. On a very simple level, ^{90}Y derived flux measurements (as shown in Table A2.3 and Fig. A2.6) can be converted into units of per capita mussel clearance rates (CR; liters per hour per mussel). If dreissenid mussels are indeed responsible for the filtration of particulate matter in the water column (and the dramatic increase in water clarity), and if mussel clearance rates that have been measured in the laboratory are indeed valid in the natural environment, then both *in situ* and laboratory clearance rates might be expected to be of a similar magnitude.

The dreissenid mussel population at the Green Can 20m station (in August 2009) is estimated at 10,000 mussels m^{-2}; which is based on a local diver-assessed population of 5000 m^{-2} (10 m deep site; H. Bootsma, personal communication, 2007), a local assessed with a ponar grab sampling device of 20,000 m^{-2} (~20 m deep site; R. Cuhel, personal communication, 2007) and the survey work of Nalepa et al. (2009; 6285 ± 1450 m^{-2} in water ≤ 30m in 2005). The per capita mussel clearance rate is then simply calculated as the ^{90}Y derived mass flux divided by the integrated (trapezoidal) mass inventory of suspended material in the water column (see Table A2.1), multiplied by the ratio of liters of water to mussels on an areal basis (i.e., 20,000 liters of water over 10,000 mussels).

The results, shown in Fig. A2.8, agree well with the laboratory results obtained by Baldwin et al. (2002), where the estimates of per capita clearance rates range from a low of 0.3 ± 0.8 liters $mussel^{-1}$ day^{-1} to a high of 8.7 ± 3.5 liters $mussel^{-1}$ day^{-1} compared to Baldwin et al.'s range of ~0.2 to 9.8 liters $mussel^{-1}$ day^{-1}.

Benthic inventories and fluxes: The hypothesis - that ^{90}Y-derived fluxes are truly measuring the short-term flux of material to the lake bed - can be tested by measuring the inventory of radionuclides on the lakebed. It is also possible to examine if the efflux of radionuclides from dreissenid mussel ejecta. Both were done using material collected on September 10, 2009 by the Bootsma laboratory. Flocculent material was quantitatively removed from a known area off a large stone surface using a large (~1.5 L) syringe. The flocculent was filtered, dried and weighed. Dreissenid mussels (n = 10) were collected, washed, and placed into a Petri dish filled with filtered lake water. After 12 hours, the mussel ejecta (feces and pseudo-feces) was filtered, dried, and weighed. Duplicates of both sample types were collected. Sample weights and measured radionuclide activities and fluxes are presented in Table A2.3.
With the information supplied in Table A2.3, it is possible to compare and corroborate fluxes and inventories in the water column and lakebed. Several examples follow:

a. The age of material collected on the lakebed on September 10 can be calculated as:

$$age = \frac{-\ln\left(AR_2 / AR_1\right)}{\lambda_Y - \lambda_{Th}} \qquad \text{(A2.11)}$$

where AR_1 and AR_2 are the $^{90}Y/^{234}Th$ activity ratios in benthic sediment and the water column (at 17 meters depth), respectively. For samples BS2 and BS3 the average age of both samples is equal to 4.6 ± 1.0 days (n = 2). This suggests that material had been accumulating on the bottom rock surface (where these samples were collected) for ~ 4.6 ± 1.0 days. Presumably, this material is periodically swept away by strong currents and a resuspension event and the $^{90}Y/^{234}Th$ "clock" is reset after each event.

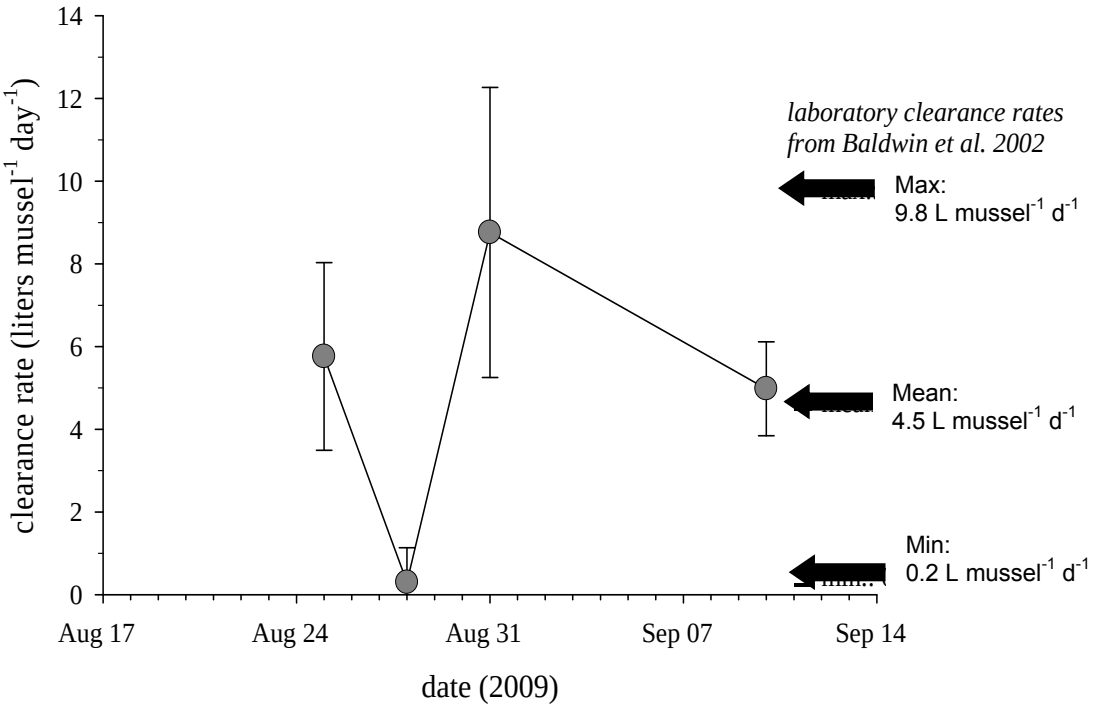

Fig. A2.8. Integrated (0-20 meter) *in situ* dreissenid mussel clearance rates derived from $^{90}Y/^{90}Sr$ disequilibria in the water column. Based on best estimate benthic population of 10,000 mussels m^{-2}. The large errors are related to low ^{90}Y activity on particulate samples. Smaller errors can be achieved with larger sample sizes. Dreissenid mussel clearance rates in the laboratory were measured by Baldwin et al. (2002).

Sample	areal floc conc $g\ m^{-2}$	areal PP conc $mg\ m^{-2}$	^{90}Y inventory $dpm\ m^{-2}$	^{234}Th inventory $dpm\ m^{-2}$
BS2	182	140	560 ± 1510	2360 ± 50
BS3	311	239	820 ± 2570	4750 ± 90

Sample	mussel ejecta $\mu g\ mussel^{-1}\ hr^{-1}$	^{90}Y flux $dpm\ mussel^{-1}\ hr^{-1}$	^{234}Th flux $dpm\ mussel^{-1}\ hr^{-1}$
ME1	16.0	1.0E-03 ± 4.7E-04	2.2E-04 ± 5.2E-06
ME2	34.9	3.6E-03 ± 1.8E-03	1.1E-03 ± 2.8E-05

Table A2.2. Benthic sediment/flocculent (BS) and mussel ejecta (ME) samples collected on September 10, 2009. BS sample inventories scaled up to 1 square meter. ME rates scaled to per capita flux. Large errors associated with BS and ME radionuclide measurements due to very low activity and associated counting errors.

b. If the ^{90}Y-derived mass flux of material from the water column (i.e., 32 ± 7 $g\ m^{-2}\ d^{-1}$ on September 10; from Table A2.2) is multiplied by the average age of material on the bottom (i.e., 4.6 ± 1.0 days), a benthic sediment inventory is estimated:

   $32 \pm 7\ g\ m^{-2}\ d^{-1} * 4.6 \pm 1.0\ days = 147 \pm 45\ g\ m^{-2}$

   which (from Table A2.3) is reasonably close to the measured benthic sediment inventory of 247 ± 91 $g\ m^{-2}$ (i.e., the average of BS2 and BS3 measurements) and certainly much more close than either the ^{234}Th or sediment trap derived estimates which are roughly ~ 1 $g\ m^{-2}$ and ~0.4 $g\ m^{-2}$, respectively (Fig. A2.9a).

c. The same calculation can be applied to particulate phosphorus. If the ^{90}Y-derived particulate phosphorus flux of material from the water column (i.e., 104 ± 24 $mg\ m^{-2}\ d^{-1}$ on September 10; from Table A2.2) is multiplied by the average age of material on the bottom (i.e., 4.6 ± 1.0 days), the estimated benthic particulate phosphorus inventory is:

   $104 \pm 24\ mg\ m^{-2}\ d^{-1} * 4.6 \pm 1.0\ days = 480 \pm 150\ mg\ m^{-2}$

   which (from Table A2.3) is approximately double the measured benthic sediment inventory of 190 ± 70 $mg\ m^{-2}$ (i.e., the average of BS2 and BS3

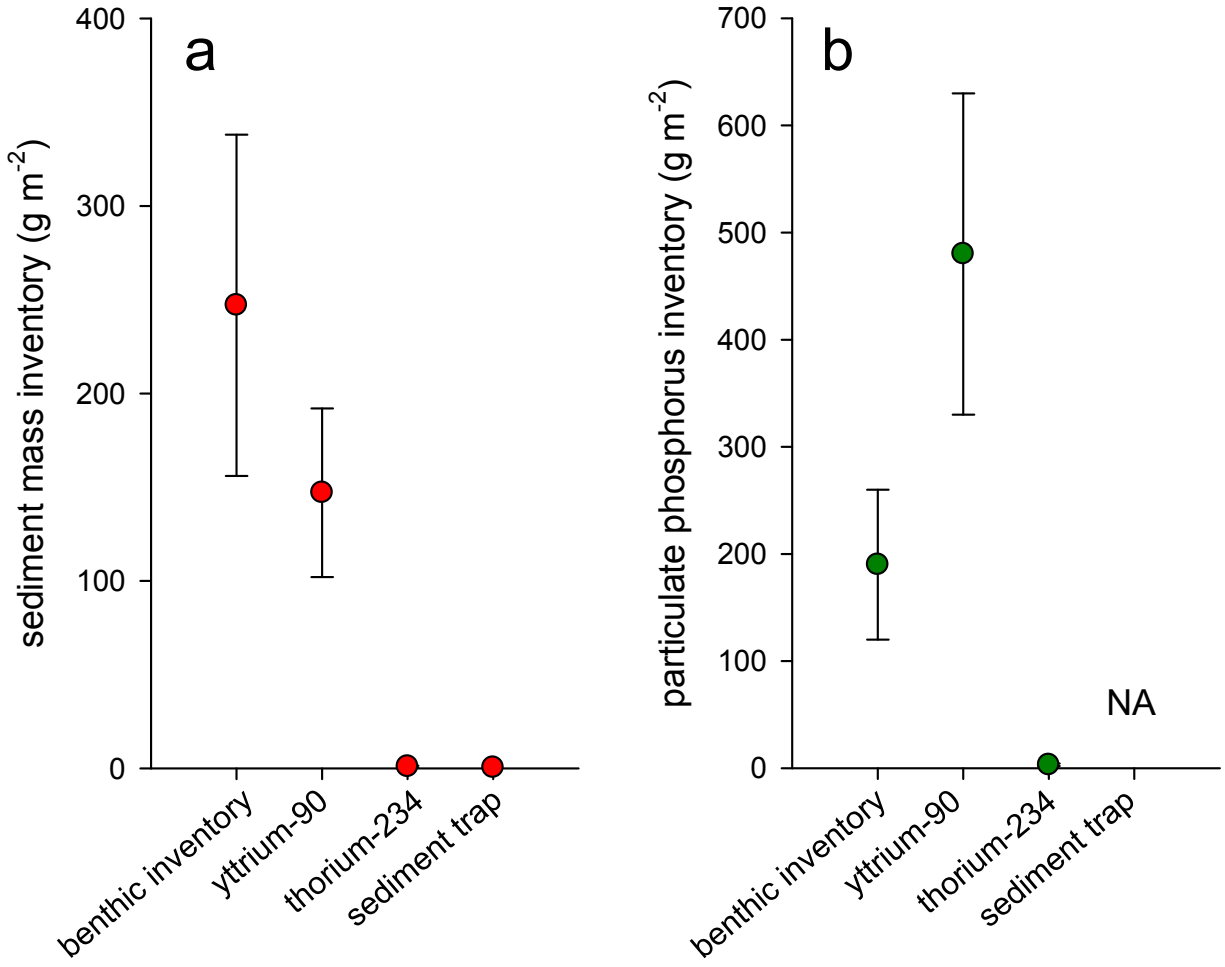

Figure A2.9. (a) measured (benthic inventory) sediment mass versus calculated benthic inventory mass based on estimates derived from the ^{90}Yand ^{234}Th tracers and a sediment trap. (b) – measured (benthic inventory) particulate phosphorus versus calculated benthic inventory particulate phosphorus mass based on estimates derived from the ^{90}Y and ^{234}Th tracers.

measurements). By comparison, the ^{234}Th derived estimate of the benthic particulate phosphorus inventory is roughly ~ 3 mg m^{-2} (Fig. A2.9b). The errors on the fluxes are admittedly high, however, it is intriguing that the ^{90}Y-derived estimate of particulate phosphorus flux is approximately twice as high as what is found on the bottom rock surface. Can the missing phosphorus be accounted for by mussel (and/or other biotic) uptake?

d. If the measured flux of ^{234}Th from the water column on September 10 (i.e., 12.9 ± 4.0 dpm m^{-2} d^{-1}, from Fig. A2.2) is multiplied by the average age of material on the bottom (i.e., 4.6 ± 1.0 days), the estimated benthic ^{234}Th inventory is:

   12.9 ± 4.0 dpm m^{-2} d^{-1} * 4.6 ± 1.0 days = 59 ± 22 dpm m^{-2}

   which (from Table A2.3) is substantially less than the measured benthic ^{234}Th inventory of 3600 ± 1700 (i.e., the average of BS2 and BS3 measurements). This does not imply that the measured flux of ^{234}Th from the water column is incorrect. Rather, it points to the fact that a water mass with higher ^{234}Th activity has moved over the sampling station location. Indeed, if the benthic ^{234}Th inventory (i.e., 3600 ± 1700 dpm m^{-2}) is added to the water column ^{234}Th inventory (2750 ± 30 dpm m^{-2}) the total (benthic plus water column) inventory is 6400 ± 1700 dpm ^{234}Th – which is somewhat higher than the parent inventory of 4600 dpm m^{-2} ^{238}U.

e. Finally, the average measured flux of ^{90}Y and ^{234}Th from mussels (i.e., 0.0023 ± 0.0018 dpm ^{90}Y mussel^{-1} hr^{-1} and 0.0007 ± 0.0006 dpm ^{234}Th mussel^{-1} hr^{-1}, from Table A2.3) is multiplied by the estimate of mussel density on the lakebed (i.e., 10,000 mussels m^{-2}) to get mussel ejecta fluxes of 550 ± 440 dpm ^{90}Y m^{-2} d^{-1} and 160 ± 150 dpm ^{234}Th m^{-2} d^{-1}. These estimates tend to be slightly less than the measured water column flux of ^{90}Y (i.e., 1270 ± 140 dpm ^{90}Y m^{-2} d^{-1}) and greater than the measured water column flux of ^{234}Th (i.e., 13 ± 4 dpm ^{234}Th m^{-2} d^{-1}). However, given the general uncertainty in mussel population density (~ factor of 2), the large errors associated with the radionuclide measurements (due to low activities, small sample sizes, and propagated counting errors), and the unknown changes to mussel ejection rates in the laboratory, these comparisons are reasonable.

Summary and Conclusions

- Over the course of this study (August 20 to September 10, 2009), mass and particulate phosphorus fluxes were measured at a 20-meter deep station in southwestern Lake Michigan using two radionuclide tracers (^{234}Th and ^{90}Y) and a sequencing sediment trap (located at 10 meters depth).

- Measured mass fluxes were lowest with the sediment trap. However, strong water currents appeared to cause an oversampling bias. Some of the difference in sediment trap versus radionuclide-derived fluxes can be attributed to the inability of a sediment trap to measure particle interception in a mixed water column.

- ^{234}Th-derived fluxes were generally an order of magnitude smaller than ^{90}Y-derived fluxes. This is attributed to the longer half-life of ^{234}Th (24.1 days versus 64 hours for ^{90}Y). The ^{234}Th tracer has been shown to be a good indicator of offshore transport in Waples et al. (2004) and operates on a time-scale of days to weeks. The ^{90}Y tracer, on the other hand, measures particle dynamics on a time scale of hours to days. Hence the ^{90}Y-derived results presented here provide information on how particle and phosphorus movement between the water column and the benthos (lake bottom) in the nearshore zone change from day to day. These measurements are then directly comparable with those obtained from the benthic chamber experiments and PIV deployments, which also represent short time periods.

- ^{90}Y-derived fluxes of suspended matter (from the water column) ranged from a low of 2 ± 5 g m^{-2} d^{-1} on August 28 to a high of 68 ± 27 g m^{-2} d^{-1} on August 31. ^{90}Y-derived fluxes of particulate phosphorus ranged from a low of 8 ± 22 mg m^{-2} d^{-1} on August 28 to a high of 235 ± 94 mg m^{-2} d^{-1} on August 31.

- ^{90}Y-derived mass fluxes were converted into estimates of dreissenid mussel clearance rates (CR). Comparisons of ^{90}Y-derived CR estimates over the course of the sampling period agreed well with laboratory measurements of CR made by Baldwin et al. (2002).

- Measurements of benthic (sediment) inventories of ^{90}Y and ^{234}Th tended to support the estimates of ^{90}Y-derived fluxes from the water column.

- Measurements of ^{90}Y and ^{234}Th flux from collected dreissenid mussels were reasonably close to measured radionuclide fluxes from the water column (i.e., within a factor of 2). Faster sample processing and larger sample sizes are needed to reduce the propagated errors in these estimates.

Appendix III. Nearshore – Offshore Exchange in the Milwaukee Region of Lake Michigan

Introduction

The primary goal in studying nearshore – offshore exchange was to determine the extent to which energy flow and nutrient dynamics within the nearshore zone are influenced by pelagic (offshore zone) processes. From a nutrient management perspective, a particularly important question is: to what degree do nearshore biota rely on nutrients derived from the pelagic zone? A number of recent publications (Zhu et al. 2006; Hecky et al. 2004) have proposed that dreissenid mussels (zebra mussels and quagga mussels) have altered the nutrient cycling processes in lakes by removing nutrients (in the form of plankton) from the pelagic zone and concentrating these nutrients within the nearshore zone. This nutrient concentration mechanism may in turn be responsible for the excessive growth of *Cladophora* and other benthic algae, such as *Chara*, *Spirogyra*, *Zygnema* and *Mougeotia* that have been observed in parts of Lake Michigan and other Great Lakes. If this is indeed the case, it has important implications for *Cladophora* management strategies. The primary nutrient management tool that has been applied in the Great Lakes over the past four to five decades is reduction in nutrient loading from tributaries, which is achieved through several initiatives, including improved agricultural practices, efforts to limit runoff in both rural and urban environments, and restrictions on nutrient discharge from industry and waste water treatment plants. **If nearshore algae are now obtaining a significant proportion of their phosphorus from the pelagic phosphorus pool, which is several times larger than the annual phosphorus load to Lake Michigan, the efficacy of nutrient load reductions may be severely limited, especially over the short term.**

The nearshore zone defined in our research can be considered as a part of the coastal boundary layer (CBL) from the perspective of coastal hydrodynamics (Csanady 1972; Rao and Schwab 2007). The flow direction in a CBL is predominately parallel to the coastline. Thus the advective exchange between nearshore and offshore zones is limited. However, several hydrodyamic processes, including coastal upwelling / downwelling, internal waves, eddy diffusion, and horizontal advection, can lead to cross-shore transport that results in transport of water and nutrients between the nearshore and offshore zones. These exchange processes can vary dramatically over space and time, making it very difficult to directly measure exchange using in-lake instruments.

FVCOM Model Simulations

Numerical models are a powerful tool to examine nearshore hydrodynamic processes, because they allow for a thorough analysis of temporal and spatial structure. We adapted an unstructured-grid Finite-Volume Coastal Ocean Model

(FVCOM; Chen et al. 2003) to simulate the hydrodynamic circulation of Lake Michigan. The model was set up with an average horizontal resolution of 3 km and nearshore resolution of 1.5 km. This model allowed us to determine nearshore-offshore exchange rates integrated over various temporal and spatial scales.

Prior to using the model for this purpose, it was necessary to validate it against empirical data. Fig. A3.1 provides a comparison of FVCOM-simulated current speeds and directions with empirical data collected with an acoustic Doppler current profiler (ADCP) deployed at the Green Can study site. The figure illustrates a generally good agreement in the magnitude, direction, frequency and phase of coastal currents, validating the use of the model to examine nearshore hydrodynamics and nearshore-offshore exchange.

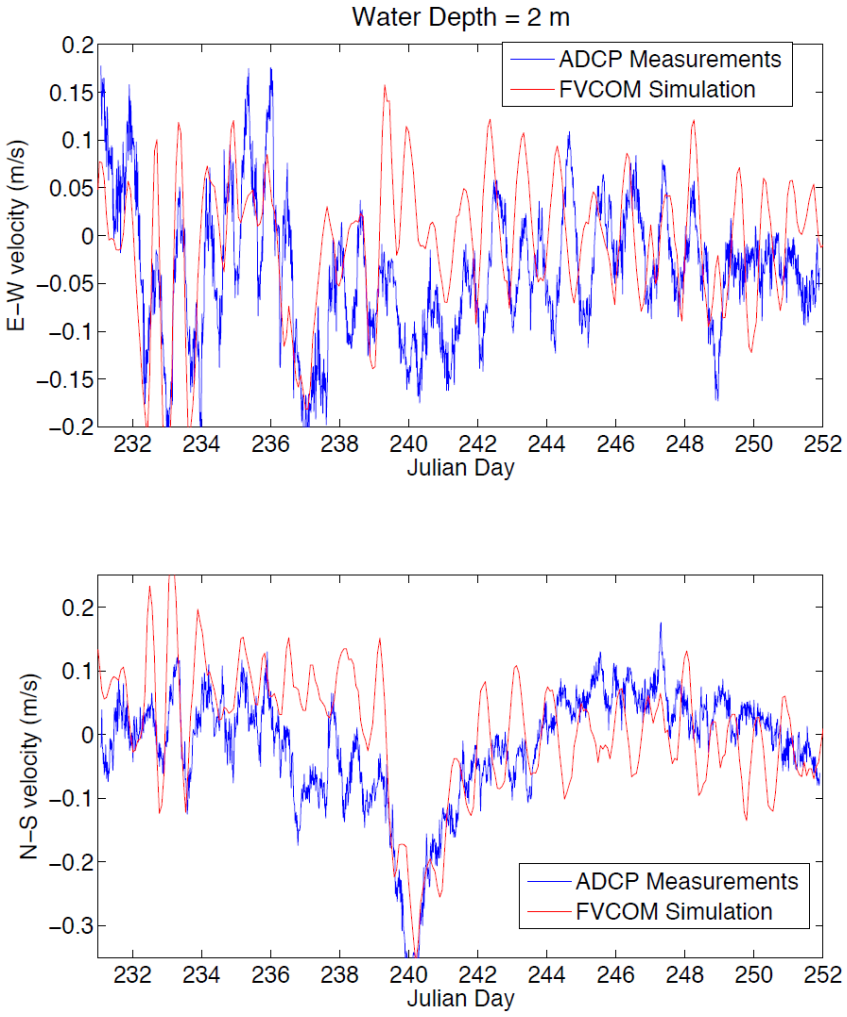

Fig. A3.1. Measured and simulated current speeds and directions over a 3-week period at the Green Can study site in 2009. The upper graph presents current velocities along the east-west axis (east is positive, west is negative), and the lower graph presents velocities along the north-south axis (north is positive).

Fig. A3.2. shows depth-averaged currents for the lakeshore region from Racine to Sheboygan. The model results demonstrate the variability of currents in both the pelagic and nearshore zones. On the date shown, nearshore currents were parallel to shore in most regions, but between Atwater and Sheboygan the current direction was southward, while it was northward between Milwaukee and Racine. A convergence zone just north of Atwater resulted in offshore transport, while onshore transport was apparent near Sheboygan and Racine.

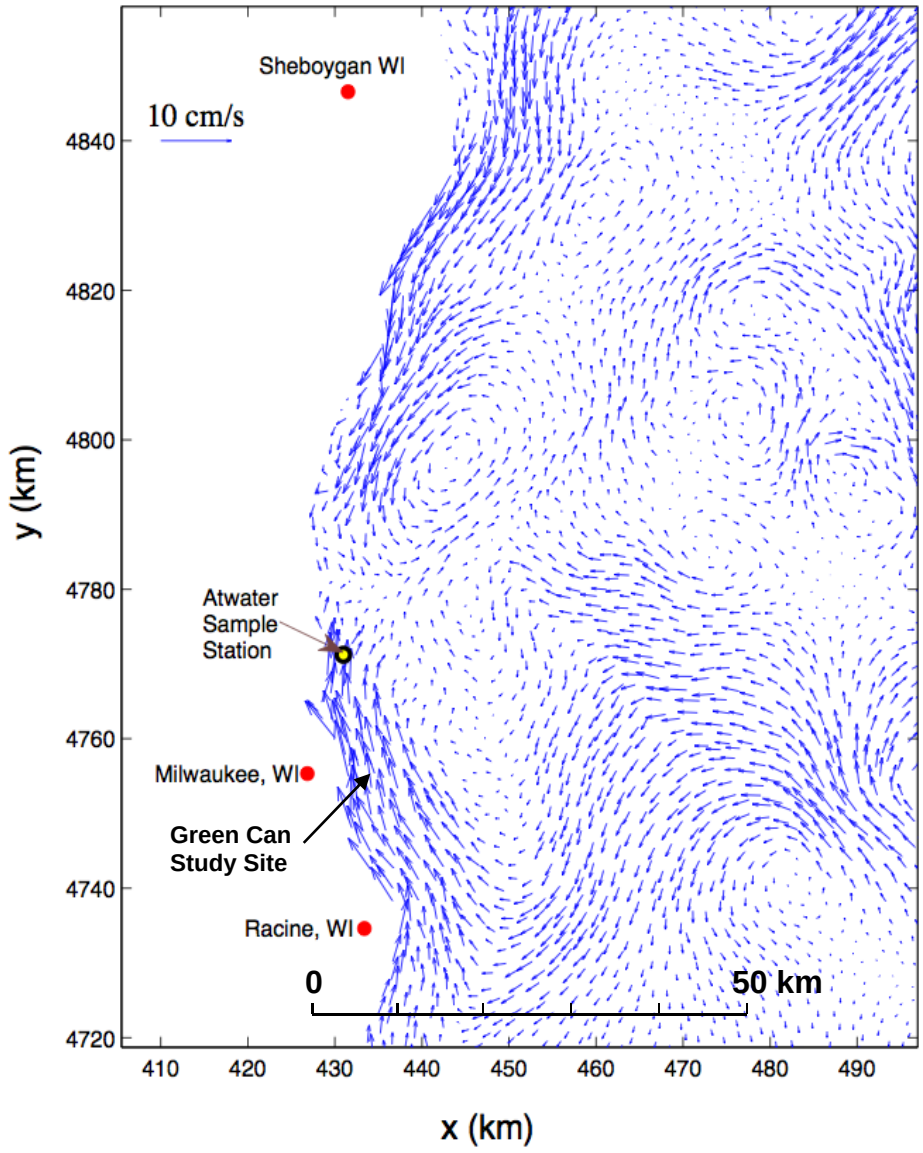

Fig. A3.2. FVCOM coarse resolution simulation results for May 18, 2009. Note the high degree of heterogeneity in nearshore currents, including coastal gyres, and zones of both onshore and offshore advection.

Results of a high-resolution simulation for the months of September and October 2009 are shown in Fig. A3.3. These results, as well as those shown in Fig. A3.2, illustrate how nearshore currents can differ significantly from the larger scale offshore circulation patterns. For example, in September the prevailing current direction 5 to 8 km offshore (region circled in figure) is southward, but the prevailing current closer to shore is northward, and complex gyres are visible immediately next to the Milwaukee Harbor breakwall.

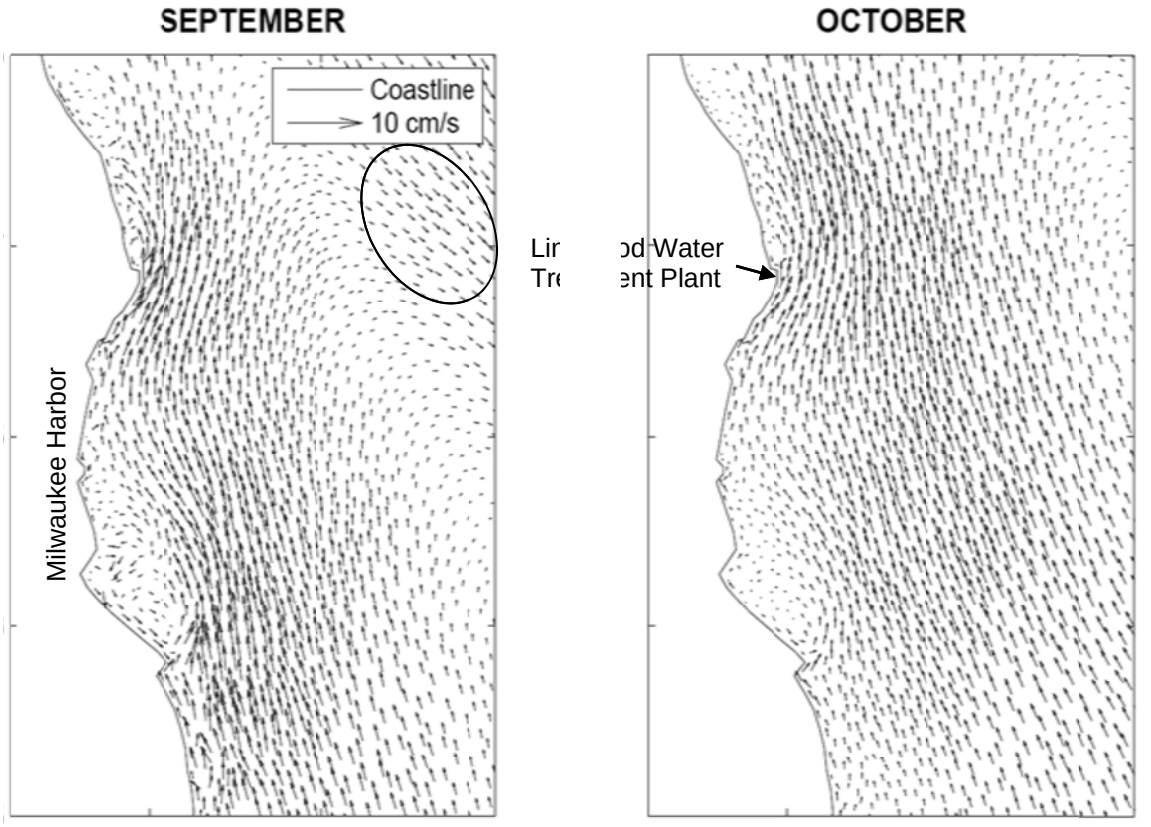

Fig. A3.3. High resolution FVCOM simulation results for the Milwaukee region, averaged for the months of September and October, 2009.

Nearshore-Offshore Exchange Estimates

To determine the magnitude of nearshore-offshore exchange, a 50 km stretch of shoreline extending from Wind Point in the south to just north of Fox Point was selected (Fig. A3.4). Within this region, a volume of water was delineated, with boundaries defined as the shoreline to the west, the northern and southern ends of the selected region, and the 20 m isobath to the east (Fig. A3.5). This control volume defines three surfaces lake waters can flow through, one in the north of the control volume, another in the south and a third in the east.

In order to quantify the relative importance of this mass exchange (E), the computed velocity field at the closest node to each surface is used to calculate the discharge going through each surface defining the control volume by determining the product between the velocity field $Vn(u,v,w)$ and a unit vector u_n pointing out of each n segment composing the surface as expressed by equation A3.1. The exchange of mass through each surface is then defined as the absolute value of the calculated discharge, multiplied by the segment width w of each segment and the height h of each sigma layer j.

$$E_{face} = \frac{\left| \sum_{i=1}^{n} \sum_{j=1}^{20} (V_{ij} u_{ij}) w_i h_j \right|}{FaceArea} \qquad \text{(A3.1)}$$

Exchange was calculated for each of the three vertical surfaces that define the control volume. Exchange was determined at several different depth interfaces by varying the isobath that defines the closure of the volume in the eastern boundary from 15 m to 60 m in increments of 5 m.

Once exchange has been calculated for each of the three surfaces defining the control volume, the relative importance of nearshore-offshore exchange is calculated as an exchange ratio:

Exchange ratio = (Cross-shore exchange) / (Along-shore exchange) (A3.2)

Here, the cross-shore exchange is defined as the exchange of mass occurring across the eastern face (i.e. between the nearshore and offshore zones). Similarly, along-shore exchange is defined as the sum of the absolute exchange calculated on the north and south interfaces. If the exchange ratio approaches unity, along-shore and cross-shore exchanges are of the same order of magnitude, implying that significant interaction between coastal and deep waters occurs. Alternatively, if the ratio approaches zero, most of the water crossing the control volume surfaces is traveling along the coast, with little interaction with deep waters.

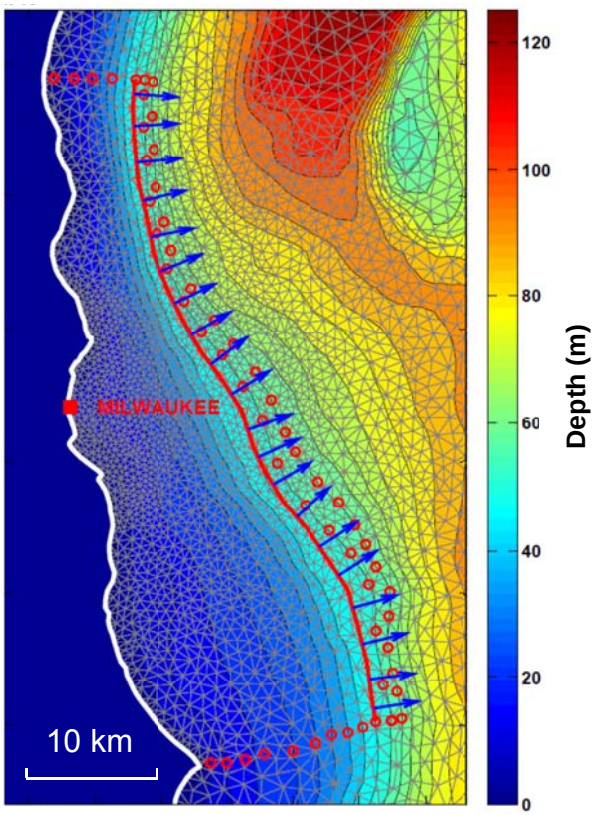

Fig. A3.4. Plot showing nearshore bathymetry, model grid, and the 20 m isobath across which nearshore-offshore exchange was calculated.

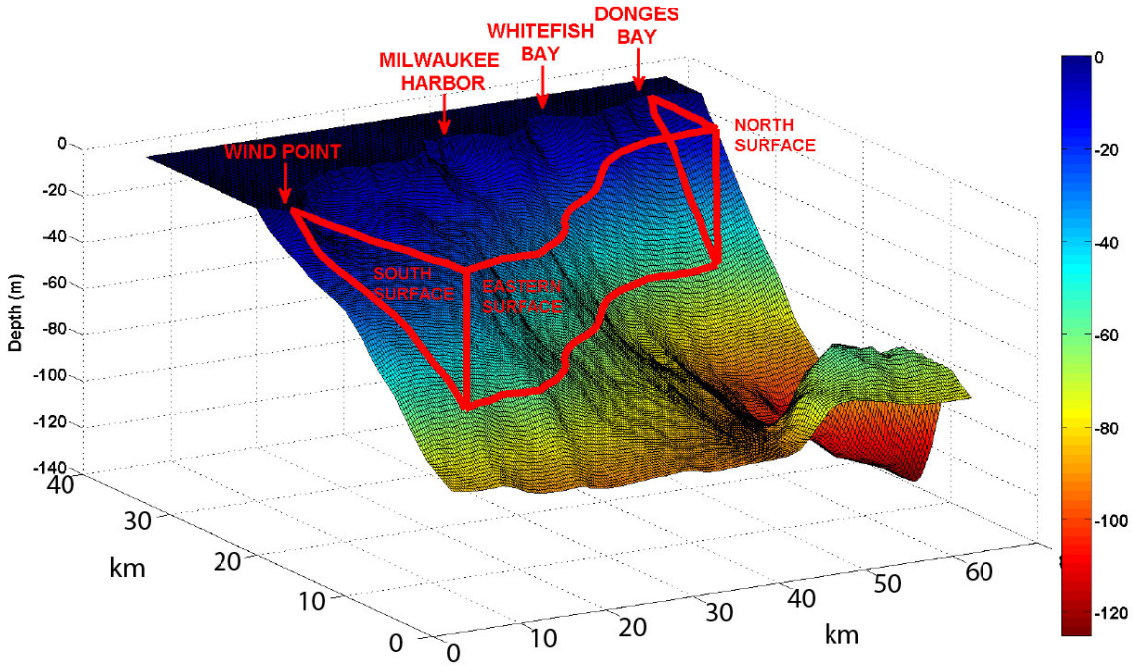

Fig. A3.5. 3-dimensional plot of the Milwaukee nearshore region, showing the nearshore volume for which nearshore-offshore (i.e. cross-shore) exchange was calculated.

Calculated exchange ratios for the period May through October, 2009, are shown in Fig. A3.6. In the spring and fall, there are moderate cross shore exchange rates, i.e. there is significant mixing between the nearshore and offshore zones. During these periods vertical stratification is weak and internal waves are less pronounced. As a result, there is little gyre formation and currents are dominated by a uniform, shore-parallel flow. However, during the summer a significant proportion of water renewal within the modeled region – sometimes more than 50% - is due to exchange with the offshore zone. Because the lake is stratified at this time, much of this exchange will occur within the epilimnion (the upper, well-mixed layer), where most phytoplankton growth occurs. Therefore these high cross-shore exchange rates may facilitate the transport of large amounts of phytoplankton from the pelagic zone to the nearshore zone, where the plankton will support mussel growth and phosphorus recycling.

The relative importance of this supply mechanism can be assessed by comparing potential flux of particulate phosphorus from the offshore zone to the nearshore zone with phosphorus loading from the Milwaukee River. Offshore – nearshore flux can be estimated according to Fick's first law of diffusion:

$$F = -D\ \delta C/\delta y \qquad \text{(A3.3)}$$

where F is flux with units of mass per area, D is the eddy diffusion coefficient,

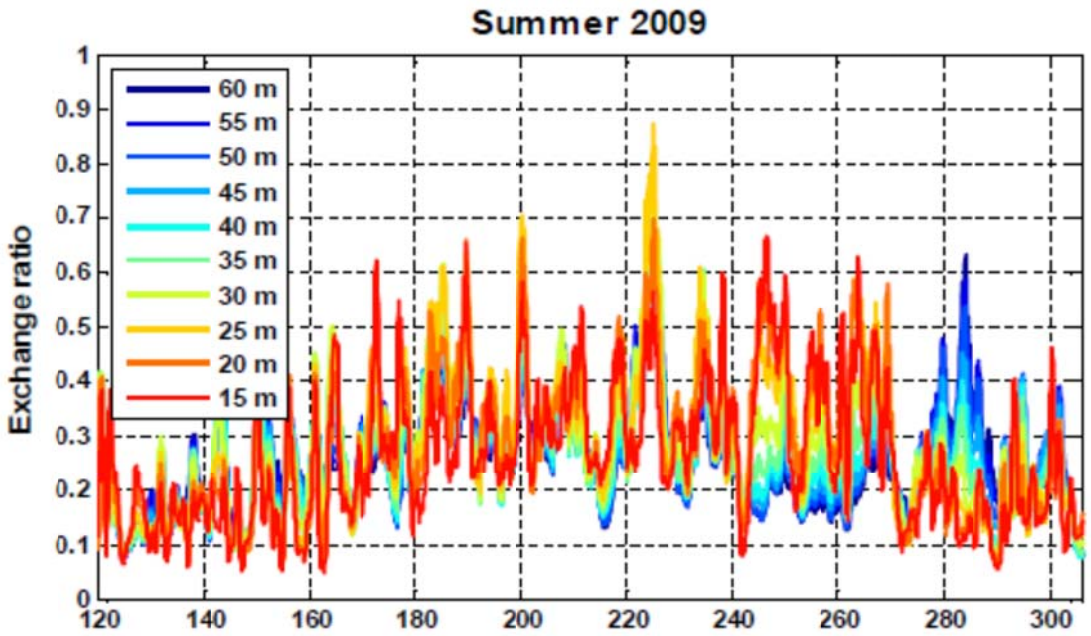

Fig. A3.6. The exchange ratio (cross-shore exchange as a proportion of along-shore exchange) determined at various distances from shore (from the 15 m isobath to the 60 m isobath) from Julian day 120 (May 1, 2009) to 304 (October 31, 2009).

and $\delta C/\delta y$ is the horizontal gradient of the concentration of particulate P. For Lake Ontario, typical cross-shore diffusion coefficients at a distance of 3 – 4 km offshore (which approximates the offshore distance of the 20 m isobath) ranged from 3.4 x 10^5 to 10.2 x 10^5 cm^2 s^{-1} (Rao and Murthy 2001). These are similar to the values observed on Lake Michigan. For the purpose of the estimates presented here, we chose a value of 6 x 10^5 cm^2 s^{-1}. Currently there is little data with which to determine the horizontal concentration gradient of particulate P ($\delta C/\delta y$). This gradient can be expected to vary to a large degree spatially and temporally, due to changes in mixing conditions that can make the nearshore zone either a net particle sink (during calm periods) or a particle source (during turbulent periods of resuspension). As an initial approach, we assume that the particulate P concentration at the nearshore-offshore boundary (here defined as the 20 m isobath) is 3 μg L^{-1}, which is a typical pelagic value for Lake Michigan, and that the concentration linearly decreases to 0 μg L^{-1} at the shoreline. Under such conditions, mussels would be consuming all of the particulate material that flows from the offshore to the nearshore zone. While the hypothetical gradient is rarely realized (shoreline particulate P is never 0, but the horizontal gradient at the 20 m isobath may actually be greater than that inferred from this assumption), the consumption rate that it represents may be realistic. If our estimated clearance rate of 3.9 L $mussel^{-1}$ day^{-1} is applied to a mussel density of 10,000 m^{-2}, the effective piston velocity (i.e. the depth of the water column that is filtered per unit time) is 39 m day^{-1}, which is nearly 4 times the average depth of the nearshore zone. In other words, the mussel community may very well be able to consume all particulate P that moves into the nearshore zone from the offshore zone.

Using the above approach, and assuming that the average width of the nearshore zone is 4 km, the calculated horizontal particulate P gradient is 0.00075 mg m^{-4}. Using this value in Equation A3.3 results in an estimated offshore – nearshore flux rate of 0.045 mg P m^{-2} s^{-1}. Note that this is a horizontal flux across the nearshore-offshore boundary. This boundary can be considered as a vertical "wall" at the 20 m isobath, separating the nearshore and offshore zones. To define this vertical flux to the lake bottom within the nearshore zone, it must be multiplied by 20/4000, which is the ratio of the vertical "wall" height to the horizontal width of the nearshore zone. This results in an estimated vertical particulate P flux rate of 19.4 mg m^{-2} day^{-1}.

This flux can be put into context by comparing it with the total phosphorus load from Milwaukee Harbor to the lake. An approximate harbor loading rate during summer is 247 kg P day^{-1} (Bootsma et al. 2008a). Translation of this value to an areal loading rate within the nearshore zone requires a specification of the length of shoreline over which this load is spread. This will vary depending on a number of factors, including nearshore currents and density of river water relative to lake water. However, even if the river load is confined to a lakeshore length as short as 3 km, which can be considered a minimum distance over which river load is deposited, the areal deposition of river-derived P within this 3 km stretch would

be approximately equal to the flux of P from the offshore zone. Outside of this 3 km stretch, virtually all P flux to the nearshore zone would be from the offshore zone. Regardless of the distance over which river loading is spread, the flux of P from the offshore to the nearshore zone appears to be similar to, or greater than, the flux from rivers for most parts of the nearshore zone.

While these estimates are based on some assumptions that require further validation, they support earlier findings that mussels are major players in the nearshore zone phosphorus cycle. They suggest that a large proportion of the phosphorus supply to the nearshore zone may be in the form of plankton that originates in the pelagic zone. Production of pelagic plankton ultimately relies on phosphorus that is loaded to the lake via the nearshore zone. **But because the pelagic plankton community represents a very large nutrient pool that is spatially diffuse and has a long turnover time, its utilization as a phosphorus source by the nearshore community means that decreases in phosphorus loading from tributaries will likely have only a marginal effect on nearshore phosphorus concentration nuisance algal abundance in the short term. As long as high mussel densities persist in the nearshore zone, significant decreases in phosphorus supply to benthic algae will only result from decreases in the size of the pelagic phosphorus pool.**

Literature References

Auer, M. T., L. M. Tomlinson, S.N. Higgins, S.Y. Malkin, E.T. Howell, and H.A. Bootsma. 2010. Great Lakes *Cladophora* in the 21st century: same algae, different ecosystem. J. Great Lakes Res. 36: 248-255.

Baldwin, B. S. , M. S. Mayer, J. Dayton, N. Pau, J. Mendilla, M. Sullivan, A. Moore, A. Ma, E. L. Mills. 2002. Comparative growth and feeding in zebra and quagga mussels (*Dreissena polymorpha* and *Dreissena bugensis*): implications for North American lakes. Can. J. Fish. Aquat. Sci. 59: 680–694.

Bootsma, H.A., E.B. Young, and J.A. Berges. 2008a. Water quality management options to control *Cladophora* growth in the Milwaukee region of Lake Michigan. Great Lakes WATER Institute Technical Report No. 2008-01(56), submitted to the Milwaukee Metropolitan Sewerage District.

Bootsma, H.A., B.T. Maybruck, S.A. Faude, and J.S. Schafer. 2008b. Modeling of thermal impacts on benthic algae. Pages 12-1 – 12-10 ***In*** Proceedings: Second Thermal Ecology and Regulation Workshop: October 2-3, 2007. EPRI, Palo Alto, CA: 2008. 1016809. Pages 12-1 – 12-10.

Bootsma, H.A. 2009. Causes, consequences and management of nuisance *Cladophora*. Report submitted to the Environmental Protection Agency, Great Lakes National Program Office. Project GL-00E06901.

Brooks, A., and D. Edgington. 1994. Biogeochemical control of phosphorus cycling and primary production in Lake Michigan. Limnol. Oceanogr. 39(4): 961-968.

Cha, Y., C. A. Stow, T.F. Nalepa, and K.H. Reckhow. 2011. Do invasive mussels restrict offshore phosphorus transport in Lake Huron? Environ. Sci. Technol.: dx.doi.org/10.1021/es2014715.

Chen, C., H. Liu, and R. C. Beardsley. 2003. An unstructured grid, finite-volume, three-dimensional, primitive equations ocean model: application to coastal ocean and estuaries. J. Atmos. Oceanic Technol. 20: 159-186.

Csanady, G.T. 1972. The coastal boundary layer in Lake Ontario. Part I: the spring regime. J. Phys. Oceanogr. 2(1): 41-53.

Fahnenstiel, G., S. Pothoven, et al. 2010. Recent changes in primary production and phytoplankton in the offshore region of southeastern Lake Michigan. J. Great Lakes Res. 36 (Suppl. 3): 20-29.

Heath, R., G. Fahnenstiel, et al. (1995). Ecosystem-Level Effects of Zebra Mussels (*Dreissena ploymorpha)*: An Enclosure Experiment in Saginaw Bay, Lake Huron. J. Great Lakes Res 21(4): 501-516.

Hecky, R. E., R. Smith, et al. (2004). The nearshore phosphorus shunt: a consequence of ecosystem engineering by dreissenids in the Laurentian Great Lakes. Canadian Journal of Fisheries and Aquatic Sciences 61: 1285-1293.

Kling, G.W., K. Hayhoe, L.B. Johnson, et al. 2003. Confronting climate chagne in the Great Lakes region: impacts on our communities and ecosystems. Union of Concerned Scientists, Cambridge, Massachusetts, and Ecological Society of America, Washington, D.C.

Liao, Q., H. A. Bootsma, et al. (2009). Development of an *in situ* underwater particle image velocimetry (UWPIV) system. Limnol. Oceanogr. Methods. 7: 169-184.

Makarewicz, J. C., P. Bertram, et al. (2000). Chemistry of the offshore surface waters of Lake Erie: pre- and post-*Dreissena* introduction (1983-1993). J. Great Lakes Res. 26(1): 82-93.

Mida, J. L., D. Scavia, et al. (2010). Long-term and recent changes in southern Lake Michigan water quality with implications for present trophic status. J. Great Lakes Res. 36 (Suppl. 3): 42-49.

Nalepa, T. F., D. L. Fanslow, G. A. Lang. 2009. Transformation of the offshore benthic community in Lake Michigan: recent shift from the native amphipod *Diporeia* spp. to the invasive mussel *Dreissena rostriformis bugensis. Freshwater Biology* 54: 466–479.

Nalepa, T.F., D.L. Fanslow, et al. 2010. Recent changes in density, biomass, recruitment, size structure, and nutritional state of *Dreissena* populations in southern Lake Michigan. J. Great Lakes Res. 36 (Supp. 3):5-19.

Pauer, J. J., K. W. Taunt, et al. (2007). Resurrection of the Lake Michigan eutrophication model, MICH 1. J. Great Lakes Res. 33(3): 554-565.

Rao, Y.R., and C.R. Murthy. 2001. Coastal boundary layer characteristics during summer stratification in Lake Ontario. J. Phys. Oceanogr. 31:1088-1104.

Rao, Y.R., and Schwab, D.J. (2007). Transport and mixing between coastal and offshore waters in the great lakes: a review. J. Great Lakes Res. 33:202-218

State of the Great Lakes. 2009. Environment Canada and United States Environmental Protection Agency. ISBN 978-1-100-14102-2. EPA 905-R-09-031 Cat No. En161-3/1-2009E-PDF.

Stoeckmann, A. M. and D. W. Garton (1997). A seasonal energy budget for zebra mussels (*Dreissena polymorpha*) in western Lake Erie. Can. J. Fish. Aquat. Sci. 54: 2743-2751.

Tomlinson, L. M., M. T. Auer, et al. 2010. The Great Lakes *Cladophora* model: development, testing, and application to Lake Michigan. J. Great Lakes Res. 36(2): 287-297.

Vanderploeg, H.A., J.R. Liebig, et al. 2010. Dreissena and the disappearance of the spring phytoplnakton bloom in Lake Michigan. J. Great Lakes Res. 36(Suppl. 3):50-59.

Waples J. T. and K. A. Orlandini. 2010. A method for the sequential measurement of yttrium-90 and thorium-234 and their application to the study of rapid particle dynamics in aquatic systems. Limnol. & Oceanogr.: Methods 8: 661-677.

Waples, J. T., K. A. Orlandini, K. M. Weckerly, D. N. Edgington, and J. V. Klump. 2003. Measuring low concentrations of Th-234 in water and sediment. Mar. Chem. 80(4): 265-281.

Wisconsin Department of Natural Resources (WDNR). 2010a. Water Quality Standards for Wisconsin Surface Waters. Wisconsin Administrative Code; Chapter NR 102.

Wisconsin Department of Natural Resources (WDNR). 2010b. Effluent Standards and Limitations for Phosphorus. Wisconsin Administrative Code; Chapter NR 217.

Zhu, B., D. G. Fitzgerald, et al. (2006). Alteration of ecosystem function by zebra mussels in Oneida Lake: Impacts on submerged macrophytes. Ecosystems 9(6): 1017-1028.